



TALLINNA TEHNIKAÜLIKOOL
TALLINN UNIVERSITY OF TECHNOLOGY

Department of Electrical Power Engineering and Mechatronics

**EFFECT OF AMBIENT TEMPERATURE ON CONDITION MONITORING
OF MACHINES USING INFRARED THERMOGRAPHY**

KESKKONNATEMPERATUURI MÕJU MASINATE SEISUNDI SEIRELE KASUTADES
INFRAPUNA TERMOGRAAFIAT

MASTER'S THESIS

MECHATRONICS PROGRAM

Student Anurag Kar
Student Code 165552MAHM
Supervisor Leo Teder

Tallinn, 2019

Appendix 3 Form of author's declaration

(On the reverse side of title page)

AUTHOR'S DECLARATION

Hereby I declare, that I have written this thesis independently.

No academic degree has been applied for based on this material. All works, major viewpoints and data of the other authors used in this thesis have been referenced.

"....." 201.....

Author:

/signature /

The thesis is in accordance with the terms and requirements

"....." 201....

Supervisor:

/signature/

Accepted for defence

"....."201.....

Chairman of theses defence commission:

/name and signature/

(Tiitellehe pöördel)

AUTORIDEKLARATSIOON

Olen koostanud lõputöö iseseisvalt.

Lõputöö alusel ei ole varem kutse- või teaduskraadi või inseneridiplomit taotletud. Kõik töö koostamisel kasutatud teiste autorite tööd, olulised seisukohad, kirjandusallikatest ja mujalt pärinevad andmed on viidatud.

“.....” 201.....

Autor:

/ allkiri /

Töö vastab bakalaureusetöö/magistritööle esitatud nõuetele

“.....” 201.....

Juhendaja:

/ allkiri /

Kaitsmisele lubatud

“.....”201.....

Kaitsmiskomisjoni esimees

/ nimi ja allkiri /

CONTENTS

FOREWORD	6
EESSÖNA	7
LIST OF FIGURES.....	8
LIST OF TABLES.....	10
LIST OF ABBREVIATION AND SYMBOLS.....	11
1. INTRODUCTION.....	12
1.1. General Overview	12
1.2. Problem Statement.....	13
1.3. Hypothesis.....	14
1.4. Objectives of the Study.....	15
1.5. Thesis Structure	16
2. THEORETICAL BASIS	17
2.1. Overview	17
2.2. Literature Review regarding Infrared Thermography for condition monitoring.....	17
2.2.1. Infrared Thermography.....	17
2.2.2. Existing procedure for condition monitoring of machines	19
2.2.3. Conclusion.....	24
2.2.4. Background of IRT in Condition Monitoring	25
2.2.5. Conclusion.....	31
2.2.6. Problems related to Condition monitoring with IRT.....	32
2.2.7. Conclusion.....	35
3. RESULTS AND ANALYSIS.....	36
3.1. Overview	36
3.2. Experimental Set-up.....	36

3.3. Results.....	43
3.4. Limitations of the Thesis work.....	50
3.5. Conclusion and Future work.....	51
4. SUMMARY.....	52
KOKKUVÕTE.....	54
REFERENCE.....	55
APPENDICES.....	60
Appendix A.1.....	60
Appendix A.2.....	61
Appendix B.....	62

FOREWORD

This thesis topic was proposed by the Chair of Mechatronics. Condition monitoring of machines using Infrared Thermography is an important industrial aspect and has received substantial attention in the extant literature. The shortcomings of this technology need to be addressed to overcome faulty predictions about machine conditions. The experiments and simulation for the research work were carried out at the Department of Electrical Power Engineering and Mechatronics Laboratory.

The author would like to extend gratitude towards the Supervisor Leo Teder for his continuous support and guidance all through the course of completing this work and towards Prof. Mart Tamre who has been a constant source of support during the tenure of this research work.

Anurag Kar
Tallinn, 2019

EESSÕNA

Lõputöö teema pakkus välja Mehhatroonika Programmijuht. Masinate seisundi seire kasutades infrapuna termograafiat on oluline tööstuslikust seiseisukohast ning see on leidnud väärtuslikku tähelepanu olemasolevas kirjanduses selle tehnoloogia puudused on esmalt käsitletud, et vältida masinate seisukorra ebaõiget hindamist. Selle uurimistöö katsed ja simulatsioon viidi läbi Elecktrotehnika ja Mehhatroonika Laboris.

Autor soovib avaldada tänu oma juhendaja Leo Tederile püsiva toetuse ja juhendamise eestkogu selle uurimistöö sooritamise vältel ning Professor Mart Tamrele, kes on olnud järjepidevaks toetuse allikaks uurimistöö käigus.

Anurag Kar
Tallinn, 2019

LIST OF FIGURES

Figure 2. 1. A Cross-sectional view of the wind turbine blade. The upper side is called the intake side and the lower side is called the pressure face. (1) And (2) represents the leading edge and the trailing edge respectively. The spar (3) which stabilizes the blade is glued together with the shell (4) [25].	21
Figure 2. 2. A Schematic diagram of Inductive Transducer [26]	22
Figure 2. 3. Structural diagram of Fiber optics Transducer [26]	23
Figure 2. 4. A Schematic block diagram of Condition monitoring using Infrared Thermography [17].	26
Figure 2. 5. IRT in the monitoring of Civil Structures. (a) Pipelines of water well being monitored with IRT. Cracks or holes in Pipelines emerges as hotspots in thermal images. (b) Floor Heating being assessed with IRT. (c) Leakage in internal pipelines is being monitored. [36]	28
Figure 2. 6. Heat image of a PCB [39]	29
Figure 2. 7. (a) Heat profile under normal working condition. (b) Heat profile due to improper gland packing [7].	31
Figure 2. 8. Heat distribution profile of the ACC units. (a) Under the windless condition in winters. (b) Under windy conditions in summer [47]	33
Figure 2. 9. Effect of wind speed on temperature measurement [15]	34
Figure 2. 10. Effect of wind direction on temperature measurement [15]	34
Figure 3. 1. (a) FLIR E50 Thermal Camera [51]. (b) FLUKE IR Thermometer [52].	37
Figure 3. 2: Experimental Setup of the simulation in Laboratory	39
Figure 3. 3. Position of the lab-stand with rubber shoe just touching the disk on the motor shaft. ...	40
Figure 3. 4. Hotspots of the Thermography obtained from the Infrared Camera. (a) At 23 °C, (b) At 34,6 °C, (c) At 41,2 °C	42
Figure 3. 5. Temperature gradient for the loaded and unloaded bearing at 23 °C	44
Figure 3. 6. Temperature gradient for the loaded and unloaded bearing at 34,6 °C	45
Figure 3. 7. Temperature gradient for the loaded and unloaded bearing at 41,2 °C	46
Figure 3. 8. Trend of ΔT at 3 different ambient temperatures	48
Figure 3. 9. Graph showing the relation between the 'rate of change of temperature' with 'ambient temperature'	48
Figure A. 1. FLIR E50 IR CAMERA [51]	60
Figure A. 2. FLUKE 62 MINI IR THERMOMETER [52]	61
Figure B. 1. FLIR ResearchIR MAX: Analysis Tools [59]	62

Figure B. 2. Table of Emissivity of various Surfaces [60] 62

LIST OF TABLES

Table 3. 1. Thermal Data at 23 °C	43
Table 3. 2. Thermal Data at 34,6 °C	44
Table 3. 3. Thermal Data at 41,2 °C	45
Table 3. 4. ΔT Specifications by the International Electrical Testing Association (NETA) Maintenance Testing Specification [30].....	47
Table 3. 5. ΔT Specification by Recommendation for a manufacturer's Motor Control Centres [33].	47
Table A. 1: FLIR E50 IR Camera Specifications [57]	60
Table A. 2. FLUKE 62 MINI IR THERMOMETER Specification [58].....	61

LIST OF ABBREVIATION AND SYMBOLS

IRT	Infrared Thermography
ROI	Region of Image
AE	Acoustic Emission
UV	Ultraviolet Rays
CM	Condition Monitoring
NDT	Non-Destructive Technique
ΔT	Temperature differential of the bearing, ($^{\circ}\text{C}$)
τ_m	Torque generated by the motor shaft, (J/rad)
F_k	Frictional Force generated by the load (rubber shoe on the lab stand) on the disk, (N)
Θ	Angular Displacement, (rad)
A_m	Measured load in Amperes, (A)
A_r	Rated Load in Amperes, (A)
ϵ	emissivity
T_{amb}	Ambient Temperature, ($^{\circ}\text{C}$)
E	Total energy emitted by an object per unit area (W/cm^2)
σ	Boltzmann's constant ($5.67 \times 10^{-12} \text{ W}/\text{cm}^2\text{K}^4$)
T	Absolute Temperature (K)
P	Energy reflected from the surface of the object and is proportional to the surrounding temperature
T	Energy transmitted through the object
I	Light Intensity of the received light (cd).
I_o	Light Intensity of the Incident light (cd).
τ_L	Proportionality factor
k	Proportionality constant

1. INTRODUCTION

1.1. General Overview

Monitoring conditions of machinery is a quintessential task in industries as it prevents process breakdown, maximize the plant availability, and reduces any associated hazards. It enables industries to avoid and point out problems in the production line thus increasing productivity and thereby annual turnover. Malfunctions like wear and tear of oil and gas pipelines, leakage in valves and pressure vessels, overheating of resistors and electrical connections, corrosion caused due to rusting in mechanical parts, loose connection in power distribution systems, and damaged contacts can often lead to catastrophe in industries. Unpredicted failures of machinery and its components may lead to major accidents and huge economic losses and thus periodic monitoring and maintenance of those machines are of prime importance. In large-scale industries, the maintenance cost can be as high as 40% of the total budget [1]. Apart from financial losses, proper maintenance of machines also prevents environmental pollution.

Temperature monitoring of machine parts and its components is one of the most essential processes among industries when it comes to measuring machine performance and maintenance. Several techniques like radiography, eddy-current testing, ultrasonic emission, acoustic emission, vibrations and torque analysis, and voltage uniformity are often used for monitoring and analyzing the performance of machines, but temperature is considered to be the most reliable evaluation parameter [2] because it is less cumbersome, the measurement process is relatively cheap, and also machine conditions can be predicted with a relatively higher degree of accuracy by analyzing the change in temperature. However several factors affect thermal data obtained from temperature sensors. Faulty data acquisition can lead to misinterpretation of thermal data thereby leading to wrong predictions of machine condition.

This thesis work aims at finding how ambient temperature affects condition monitoring (CM) of machines and its components using Infrared thermography. A thermal camera is used to acquire images of machines and its parts in real time in a non-contact and non-invasive manner at various ambient temperatures. The acquired data is then used to compare and analyze the temperature of

the region of interest and a reference region. The temperature difference between the region of interest and the reference region (ΔT) is then compared with some standard ΔT tables which consist of different priority classes with each class representing different levels of severity. [3]

1.2. Problem Statement

Several temperature measurement tools like a thermocouple, RTDs and thermistors can be used to measure temperature with a certain degree of accuracy. But the problem with these sensors are, they are in general contact type sensors and does not provide a visual image of the subject under investigation. The problem with contact type sensors is they have to be installed and monitored manually at the defect site which not only increases the risk of human exposure but also makes the maintenance of these sensors very difficult.

IRT has been successfully used for monitoring of civil structures [4], monitoring of plastic deformation [5], monitoring of PCBs [6], monitoring of machineries [7], high level current density identification [8], paper industries [9], inspection of food [10], nuclear field [11], aerospace [12] etc.

In this study, IRT has been used for monitoring temperatures of machines using an Infrared Camera in a non-contact manner. Now, data acquired from Infrared cameras are subject to various anomalies. Several factors affect readings obtained from the cameras which in turn affect the monitoring of machines and equipment. Thermal imaging obtained in a qualitative manner is affected by external factors like emissivity of the subject, ambient temperature, reflected energy from surrounding objects, wind influence, and distance from the object [13]. Key issues include reflection from surrounding objects and ambient temperature [14] [15]. Temperature measurement from infrared cameras are seriously affected by the surrounding temperature and is one of the main reasons for faulty data acquisition from IRT.

This thesis work aims at finding how ambient temperature affects thermal data while monitoring machine and machine parts using infrared thermography. A simulated environment has been created to acquire the thermal data of a DC Motor, which is the research object for this study, using the FLIR IR Camera. Qualitative data analysis was performed using the FLIR thermal camera wherein data

acquisition from a region of image (ROI) under loaded and unloaded condition was done. The thermal data of the ROI was acquired under two different conditions. Firstly the temperature value of the bearing, which was the main focus of the research object, was acquired under a normal condition wherein no external load is applied to the motor. In the second scenario, the temperature value of the same ROI was acquired, only this time with the application of an external load, which imitate an unpredicted load in the real world. The temperature of the ROIs, under both the conditions, was analyzed through the FLIR ResearchIR Tool. The temperature difference (ΔT) of the two region which is the research parameter, in this case, was calculated. An analysis was drawn to show the relation of ΔT with the machine on-time at three different background temperature.

The findings of the study will help to understand how ambient temperature affect condition monitoring of machines using Infrared Thermography. In the greater scope, it will prevent industries from making faulty predictions about machine conditions and performance thereby increasing the machine lifetime.

1.3. Hypothesis

The effect of ambient temperature in thermal data acquisition has been mentioned by researchers before. Several factors affect thermal data acquired from Infrared cameras; the emissivity of materials, variation in ambient temperature, the presence of humidity or moisture in the air, the direction of the wind, solar heating, and energy reflected from surrounding objects, etc. [15] [16]. The most influential among these factors are ambient temperature, wind speed, and reflection from surrounding objects. When measuring temperature in a qualitative manner, ambient temperature tends to impact the temperature difference between the region of interest and the reference region. This temperature difference thus varies from season to season. It is hypothesized that, this temperature differential is directly proportional to the ambient temperature i.e. as ambient temperature increases the actual temperature of the component, under the effect of sustained load, increases and similarly as ambient temperature decreases, the temperature of the component under the same load falls below the threshold of detection but still may be potentially serious. Thus this leads to faulty predictions of actual machine condition.

This thesis work only deals with how condition monitoring of machines is affected, as ambient temperature increases. Due to a controlled temperature within the laboratory room, it was a very difficult proposition to simulate the effect of decreasing ambient temperature on condition monitoring of the machine.

$$\Delta T \propto (\tau_m, -F_k\Theta, \frac{Am}{Ar}, \epsilon, T_{amb}) \quad (1)$$

Where,

ΔT = Temperature differential of the bearing, (°C)

τ_m = Torque generated by the motor shaft, (J/rad)

F_k = Frictional Force generated by the load (rubber shoe on the lab stand) on the disk, (N)

Θ = Angular Displacement, (rad)

A_m = Measured load in Amperes, (A)

A_r = Rated Load in Amperes, (A)

ϵ = emissivity

T_{amb} = Ambient Temperature, (°C)

1.4. Objectives of the Study

The basic purpose of the study is to create a simulated model capable of estimating the effect of ambient temperature on machine condition monitoring in industries using IRT. The obtained thermal data will help to understand how ambient temperature actually affect machine monitoring and that change in ambient temperature actually changes the heat signatures obtained from machines or machine components, thus interfering with proper predictions of machine conditions and performance. This is based on the idea that all objects above 0 °C or 273 K, emits electromagnetic radiations in the infrared region of the electromagnetic spectrum. A fault in a machine part causes a rise in temperature of that particular area which then can be easily detected with the help of IRT.

1.5. Thesis Structure

This thesis work is categorized into 4 chapters.

Chapter 1 gives a detailed insight into, an overview of the thesis and discusses the problem statement and the hypothesis formulated from it.

Chapter 2 gives a thorough overview of the relevant literature undertaken for this research work. The literature review part is further categorized into three sections. The first section explains the various condition monitoring techniques used in industries and concludes its drawbacks. The second section presents a detailed review about how IRT has efficiently overcome the drawbacks, experienced with contact-type sensors for condition monitoring. The third section summarises the existing problems and the ineffectiveness of IRT to predict accurately about machine condition under certain environmental factors and that ambient temperature is one such parameter.

Chapter 3 provides a detailed description of the simulation along with the results acquired, the conclusion drawn and the future scope for improvement in this area.

Chapter 4 provides a summary of the entire thesis.

2. THEORETICAL BASIS

2.1. Overview

This section gives an overview of the relevant works related to condition monitoring with the application of IRT in various fields. As mentioned before IRT has been often used for condition monitoring of machines, civil structures, PCBs etc. Various works have been done regarding monitoring machine performance using temperature as the prime parameter but the temperature sensors that have been used are mostly contact-type sensors.

Firstly a detailed description and theory of IRT have been addressed. Second, a review of the works that have been done previously on condition monitoring is explained in details. The third part emphasizes the use of IRT in condition monitoring. Finally, a brief description of the potential gap in the previous researches and how that has been addressed in this thesis work has been mentioned.

2.2. Literature Review regarding Infrared Thermography for condition monitoring

2.2.1. Infrared Thermography

- Boltzmann's law

All objects above 0 °C or 273 K radiate infrared energy proportional to their temperature in the form of electromagnetic waves in the infrared region of the electromagnetic spectrum. Boltzmann's Law describes this phenomenon with the following equation

$$E = \sigma \epsilon T^4 [15] \tag{2}$$

Where:

E = Total energy emitted by an object per unit area (W/cm^2)

σ = Boltzmann's constant ($5.67 \times 10^{-12} W/cm^2K^4$)

ϵ = emissivity

T = Absolute Temperature (K)

In this equation, the emissivity term integrates the entire electromagnetic spectrum. Practically in real life, it is not feasible to extract the entire amount of emitted energy as energy is lost in the form of absorption, some energy is lost as it is not measurable or polluted by the environment or due to the characteristics of the object. Thus the total amount of emitted energy available to us is limited.

- Kirchoff's Law

This law states that the total amount of energy coming from the surface of an object is equal to 1. Principally the total energy coming from the surface of an object may take either of the 3 forms: that emitted by the object, that reflected by the object or that transmitted through the object. Thus Kirchoff's law can be expressed as follows

$$\epsilon + \rho + \tau = 1 \quad [15] \quad (3)$$

Where:

ϵ = emitted energy which is proportional to the temperature of the object

ρ = energy reflected from the surface of the object and is proportional to the surrounding temperature

τ = energy transmitted through the object

Generally, τ is taken to be 0 for all opaque objects thus the equation becomes

$$\epsilon + \rho = 1 \quad [15] \quad (4)$$

For a perfect blackbody, the emissivity is always equal to unity. However, for all other real surfaces, the emissivity value is less than 1. In IRT the Infrared radiations emitted by a body is detected in a non-contact manner with the help of an infrared detector and using Stefan Boltzmann's law. One of the main advantages of IRT based condition monitoring is that it requires minimal instrumentations viz an

Infrared camera and a video monitoring system for visualizing and analyzing the acquired Infrared Images.

Several parameters must be considered before choosing an Infrared camera as the accuracy of predicting the temperature of an object largely depends on the sharpness and accurate thermal images obtained which in turn depends on these performance parameters. Some of these parameters are discussed below:

- Spectral range: Spectral Range of an Infrared Camera is defined as the bandwidth of the electromagnetic spectrum within which the camera will be operating. As the temperature of an object increases the thermal radiation radiated by the object are more towards the shorter wavelengths band. [17]
- Spectral Resolution: Spatial resolution of a thermal imaging device is defined as the ability of the camera to distinguish between two objects within the field of view (FOV). Better the spatial resolution of the camera better is the quality of the acquired thermal image. [17]
- Temperature Range: Temperature range signifies the minimum and maximum temperature range measurable using the thermal imaging device.
- Frame Rate: Frame rate of a camera is defined as the number of frames acquired by the imaging device per second. A Higher frame rate is preferable for monitoring moving objects or dynamic backgrounds like propagation of thermal fronts. [17]

2.2.2. Existing procedure for condition monitoring of machines

In [18] Nandi et al. discussed how MCSA or Motor Current Signature Analysis is used for fault diagnosis of machines. This technique depends on locating specific harmonics in line current. These harmonics are usually different for different types of faults. However, this technique is not suitable for machines with multiple faults as the time harmonics generated for various faults shows similar signature and hence certain faults are not detectable. This paper also discusses various types of machine faults

encountered in industries and the various techniques for their detection. Some of the most common and major electrical faults in machines are as follows [19]:

- a) Stator faults resulting in the opening of stator windings
- b) Faulty Stator connection windings
- c) Cracked or broken rotor bars
- d) Static or dynamic air gap irregularities
- e) Gearbox failure
- f) Shaft bending resulting in friction with the rotor and stator thus causing serious damage to the windings.

The symptoms of these faults result in one of the following:

- a) Unbalanced air-gap in voltage and line currents.
- b) The decrease in the average Torque
- c) Reduction in frequency
- d) Excessive heat generation.

Bearing faults which occur mostly due to normal operating internal stress caused due to vibration, bearing current, unpredicted frictional loads and eccentricity. Certain other factors like improper lubrication and improper installations also aid to the wear and damage of bearings. Yazici et al. [20] suggested an adaptive, statistical time-frequency method for detecting bearing faults. Several experiments were conducted with defective bearings and it was claimed that the experiments results successfully recognized the damaged bearings however the detection process require extensive training for data classification and feature extraction.

In [21] Kliman et al. discussed insulation failure in stator and armature of induction motor typically arising due to a minor turn-to-turn fault which is very difficult to detect and finally end up damaging the armature insulation. It is stated that almost 30-40% of all induction motor failure happens due to this. Penman et al. [22] were able to detect the turn-to-turn faults by analyzing the axial flux component of the machine by concentrically mounting a large coil around the shaft of the machine.

In [23] Tandon et al. presented a detailed review of the vibration and acoustic methods for the condition monitoring of rolling bearings. These techniques involve vibration measurement in time and frequency domain, sound measurement, shock pulse method, and the acoustic emission technique.

Bearings are a source of vibrations or noise due to defects in them. These defects arise due to a manufacturing error, improper installations or abrasive wear. The presence of defects in bearings which may be in the form of surface roughness, misalignment of races or waviness either of which causes a significant rise in the vibration level. These defects in bearings are termed as ‘distributed defects’. The analysis of these increased vibration level due to distributed defects helps to ensure the quality of the bearings.

When any solid material under mechanical or thermal stress undergoes a change or structural alteration due to the rapid release of the strain it tends to generate elastic waves which are termed as Acoustic Emission (AE). Generation of cracks, surface nonalignment, or surface roughness is some of the major sources of AE. Hence AE is considered to be an important tool when it comes to condition monitoring in a non-destructive and non-abrasive manner. The AE system consists of transducers, sensors, amplifier, and a signal processing unit. The basic difference between Acoustic signal monitoring and vibrational monitoring lies on the fact that while vibration sensors are attached directly to the target object so as to detect vibrations precisely whereas acoustic sensors are fixed with flexible glue somewhere near the target object and record sound directly. [23] [24].

In [25] Juengert et al. demonstrated the Ultrasound-Echo technique for the condition monitoring of wind turbines. Turbine blades are made up of reinforced plastic and light materials like plastic or wood. The two-halves are laminated separately and are later glued together with an effective anti UV coating outside. Since the coating is done before the two halves are linked it is not possible to check the bonds between the shell and the spar inside the blade in a non-destructive manner.

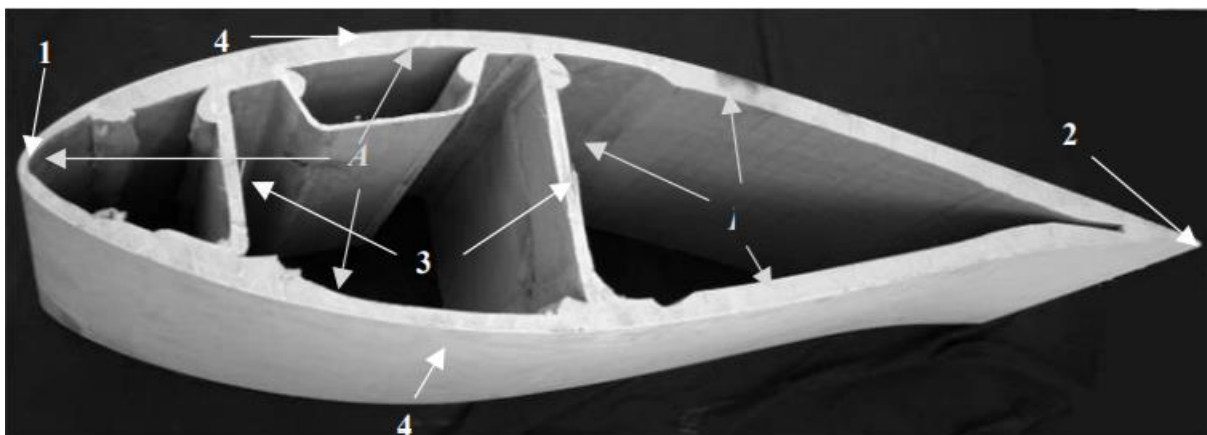


Figure 2. 1. A Cross-sectional view of the wind turbine blade. The upper side is called the intake side and the lower side is called the pressure face. (1) And (2) represents the leading edge and the trailing edge respectively. The spar (3) which stabilizes the blade is glued together with the shell (4) [25].

The Ultrasound-Echo technique is deployed for the monitoring of the bonding areas of these turbine blades. The principle is very simple. An ultrasonic pulse is sent into the materials. The waves are reflected back from the points where there is a change in material. If the shell and spar are disjointed the echo received back will arrive earlier. If there is no disjoint or the shell and spar are well bonded the echo received will be either very late or it will vanish completely.

In [26] Yin et al. describe the oil analysis method for machine condition monitoring. The paper discusses two most significant process of machine monitoring using oil analysis. Under normal condition when a machine's friction producing components is performing it produces a fairly large amount of very small wear particles approximately below the size of 10 μm . These small particles though do not produce wear but they contaminate the oil or the lubricant. These friction producing machine components slowly wear out, producing large wear particles which finally damage the system. Thus in oil monitoring, the quantity of large and small particles are usually determined. The paper discusses two types of oil monitoring process namely the inductive transducer type of oil monitoring and the fiber optics transducer type of oil monitoring. The inductive sensing technology has the capability of monitoring and sensing large wear out particles thus giving us an insight into the particular type of wear and the degree of wear. Fiber optics sensing technology is used to monitor the small wear particles suspended in the lubricant.

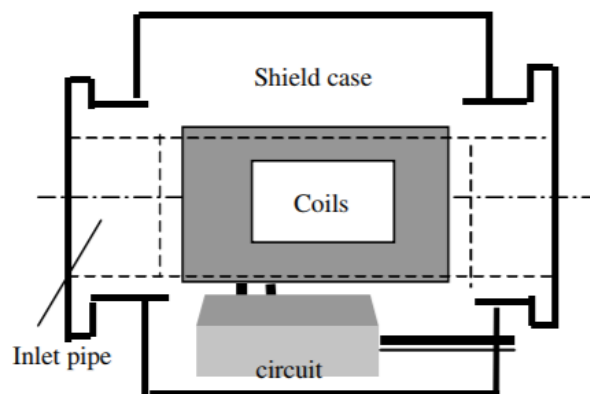


Figure 2. 2. A Schematic diagram of Inductive Transducer [26]

By the principle of electromagnetism when a conductor experiences an alternating magnetic field it produces eddy currents. When the wear particles pass through the coils it thus changes the inductance of the coil. This change in the inductance value is measured and the signal is thus analyzed to give information about the wear out particles.

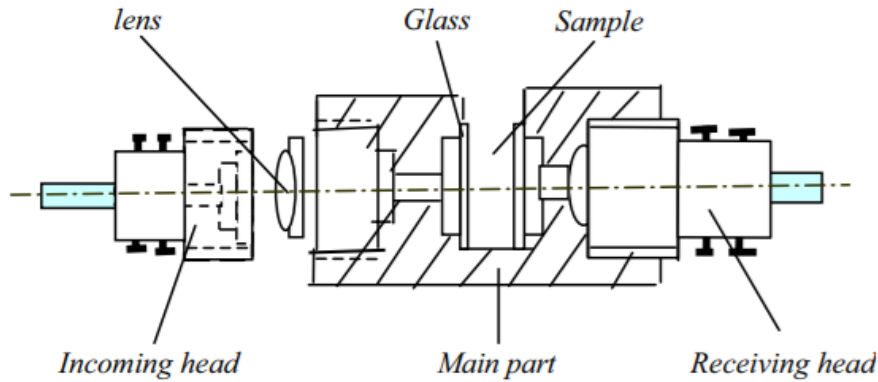


Figure 2. 3. Structural diagram of Fiber optics Transducer [26]

When a light source is passed through the oil or the lubricant the wear particles absorbs and/or scatter the lights thus reducing its intensity. The photodetector register the decrease in the light intensity due to the moving particles in the lubricant and the relation is given by Beer-Lambert's principle as follows:

$$I = I_0 \exp(-\tau_L d) \quad (5)$$

Where:

I = Light Intensity of the received light (cd).

I_0 = Light Intensity of the Incident light (cd).

τ_L = Proportionality factor

d = Length of the light path (m).

CM of machine components and equipment like motors and generators are typically performed using voltage and current analysis [24]. A spectral analysis of stator currents in generators can be used to detect cable faults [27]. The system under discussion uses an artificial neural network to learn the spectral characteristics of an operating motor in good condition. This spectrum which has harmonics of various frequencies is then passed through a filter such that only those target frequencies required for fault detection remain. The neural network system is then trained with this spectrum. After a sufficient amount of training the system is then potentially able to distinguish any different cluster of the spectrum generated by the working motor for a significant amount of time and thus is able to detect faults easily.

In [28] Louis Moranda discusses a technique called the shock Pulse Method (SPM) which is commonly used for bearing monitoring. Shock pulses in the form of transient waves are generated when a ball or roller in a bearing are rotating, throughout the life cycle of the bearing. The intensity and the waveform characteristics are directly proportional to the mechanical condition or the mechanical state of the bearing. Any discrepancies or damage to the bearing will be represented in the form of marked change in the shock pulse intensity. These shock pulses or transient waves are converted to their corresponding analog signals through pressure transducers which are installed in close vicinity to the bearings.

2.2.3. Conclusion

From the above section, the basic conclusion to be drawn is that all the above-mentioned techniques use sensors and transducers to interpret the mechanical failure or damage to the machines. The problem with these sensors are, they have to be installed somehow within close vicinity of the target area within the machines which sometimes proves costly or the process has to shut down, as recording data with certain sensors on-line is not feasible. In acoustic signal monitoring for machine performance estimation, the acoustic sensors are typically placed near the target area for recording sound whereas the vibration sensors for monitoring the vibrations from the machine components have to be placed directly with the target object to record the precise change in vibration. In the case of ultrasound-echo technique the ultrasonic sensors cannot function on-line and thus the process has to be shut down for the proper maintenance of the machines. Other available techniques for condition monitoring which do not require sensors to be installed and can record data online, are either less accurate or are not just good enough to meet the required standard.

Firstly to install these sensors manually the machines have to be shut down. In large scale industries shutting down process often proves very costly as it interferes with the continuous manufacturing process thus incurring huge economic losses. Secondly, the risk of human exposure to the machines and on-line processes can often lead to injuries and even loss of life. Thirdly the installation of the sensors near the target area in the machines often proves to be critical due to lack of apt space. Often the mechanical structure of a machine becomes a huge setback for industries to suitably installing the transducers near the target area. As a result, they either end up installing the sensors in areas from

where the signals received for analysis are weak even after proper amplification or they had to de-fabricate the machine and its components to manually install the sensors near the target area which often proves to be costly.

2.2.4. Background of IRT in Condition monitoring

The drawbacks of using contact type sensors for condition monitoring and the urgency of industrial machine maintenance gives way to IRT for performance monitoring of machines. The origin of IRT and its application for condition monitoring though came a long time ago. But it was the drawbacks of using these contact type sensors that paves the way for IRT in condition monitoring. The theory and principle of IRT have been described in detail in section 2.2.1. All objects above 0 °C (273 K) emits electromagnetic radiation in the infrared region of the electromagnetic spectrum. This infrared radiation when detected through suitable Infrared cameras gives us an account of the temperature of the body. Any fault or defect in the machine appears as a separate heat profile in a thermal image. IRT can be classified into 2 major categories- active and passive IRT [17]. This thesis work is based on passive thermography in which the object under investigation itself acts as the heat source. The temperature of the object is recorded without the influence of any external heat source.

Passive thermography is used in a wide variety of fields like structural health monitoring, medical surveillance, machinery, electrical components monitoring, mechanical deformations etc. In all the above-mentioned applications external heating is not required as the defective area or regions appears as hot spots on Infrared images with sufficient temperature difference between the defective and the non-defective region. The figure below gives a schematic view of passive thermography in a nutshell.

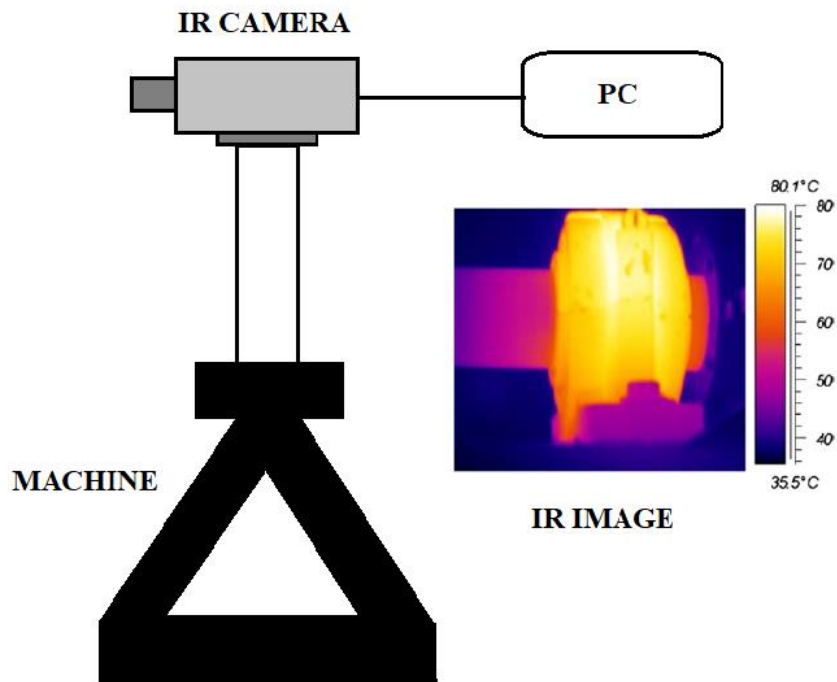


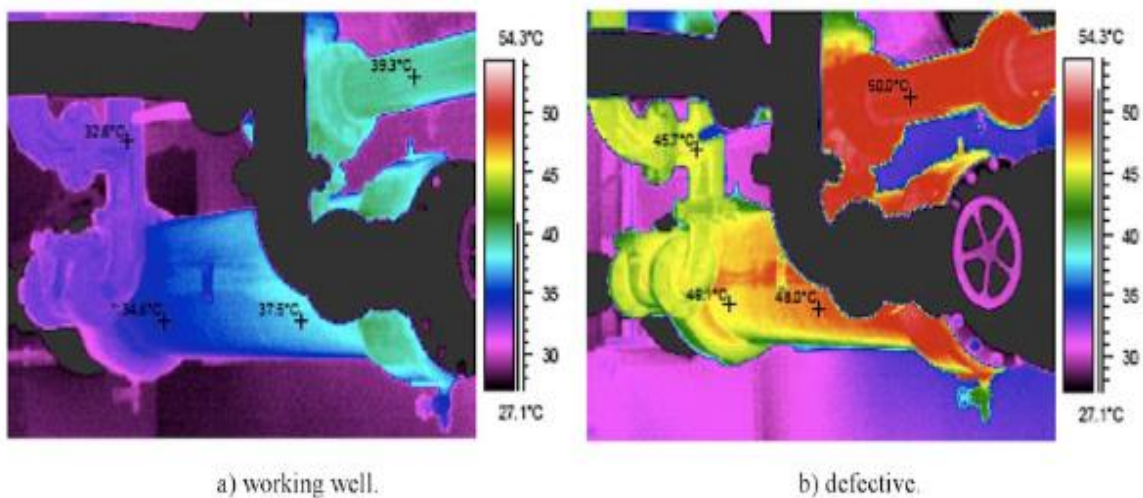
Figure 2. 4. A Schematic block diagram of Condition monitoring using Infrared Thermography [17]

Basically, there are two types of data analysis methods by condition monitoring namely a quantitative analysis method and a qualitative analysis method. In quantitative analysis method of IRT, the acquired data is used to accurately determine the temperature of a certain region, whereas in qualitative analysis relative temperature value of a local hot-spot with respect to the temperature of a reference region is compared and represented in the form of temperature differential also known as the (ΔT) criterion [29]. The severity of a situation is represented in the form of ΔT . Higher the temperature difference more severe is the case. Several standards are available which provide a detailed tabulation of (ΔT) for qualitative measurement of temperature using IRT. These tables provide a reference with each having three to four different priority classes with each class representing a particular level of severity. Some of the commonly used standards are International Electrical Testing Association (NETA) [30], American Society for Testing and Materials (ASTM) [31], National Fire Protection Association (NFPA) [32], Allen-Bradley Motor Control Standard [33]. The maximum allowable temperature for several mechanical and electrical components (bearing, rolling elements, lubricants, grease, coils, high voltage resistors, inductors, gear drives, chains, etc.) are mentioned in these standards.

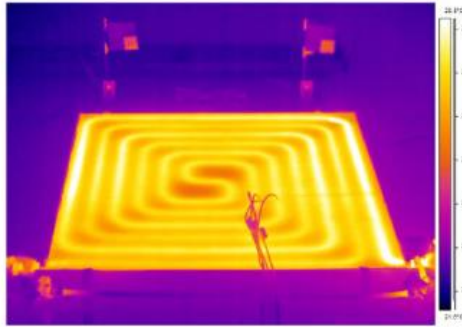
The use of IRT in the industrial application has become pretty much obvious considering the fact that it requires fewer instruments and can be used on-line without terminating the ongoing process. Moreover, temperature measurements for CM have become the most important aspect as abnormal temperature behavior and patterns and on-line measurement of temperatures in a non-contact way gives IRT an edge over other condition monitoring processes.

As mentioned before IRT has been used for condition monitoring in various fields starting from structural health monitoring, medical surveillance, machinery, aeronautics, nanostructures etc.

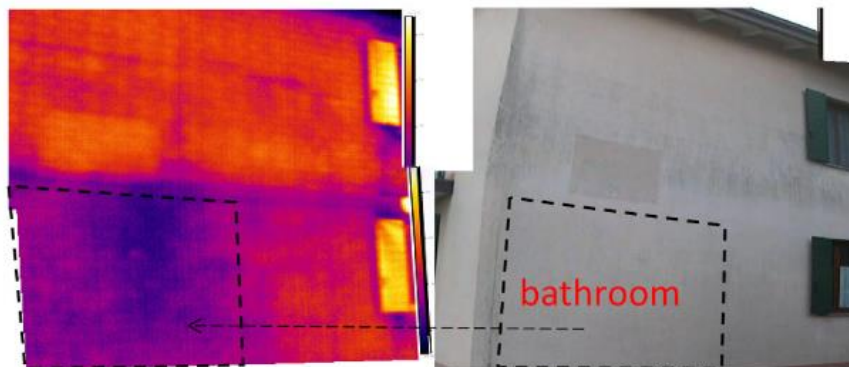
Civil structures like buildings, dams, bridges, roads etc. are an essential part of our life and periodic monitoring of these structures are very important as damaged structures can often be catastrophic leading to casualties. In [34] Ljungberg described the application of IRT in monitoring indoor and outdoor building structures, heating network, sewage systems, pipelines, and canals. The presence of cracks or voids, moisture entrapment, loose mechanical joints, wall bonding, electrical insulation in buildings can be easily detected through IRT as any crack or damage appear as bright spots in a thermal image easily distinguishable from the rest of the undamaged parts. In [4] Clark et al claimed that the nominal temperature difference between a damaged and undamaged part in an IRT induced diagnosis of building structures can be of the range of 0,2-0,3 °C. Azenha et al used IRT to monitor the early stage hardening of concrete. Hardening of concrete is an essential part when it comes to the safety and proper alignment of bricks during concrete casting and the use of IRT can be very helpful to monitor a large surface area in a non-contact manner [35]



(a)



(b)



(c)

Figure 2. 5. IRT in the monitoring of Civil Structures. (a) Pipelines of water well being monitored with IRT. Cracks or holes in Pipelines emerges as hotspots in thermal images. (b) Floor Heating being assessed with IRT. (c) Leakage in internal pipelines is being monitored. [36]

IRT has been extensively used in the condition monitoring of electrical components where faults such as corrosion, loose connections, load imbalance, damaged contacts etc. causes an abnormal rise in temperature in certain electrical components making them easily detectable by Infrared cameras. The normal operating temperature of the electrical components serve as the base temperatures for the components and a rise in temperature above that base temperature may be considered as an indication of probable failure. In [37] Newport mentioned several causes for temperature rise in electrical components which includes loose joint connections across electrical resistance, increased load (I^2R heating), eddy current heating etc.

In [13] Martinez et al. classified faults in electrical connections in three main categories based on case studies they did from 1999-2005. The three categories are serious (overheating > 130 °C), priority (overheating 100-130 °C) and programmed (overheating 70-100 °C). They also reported that 48% of

faults are found in bolted connections and 45% faults happen to be in electrical contacts. They suggested that the corrected maximum allowable temperature ($T_{max_{corr}}$) can be calculated through

$$T_{max_{corr}} = \left(\frac{A_m}{A_r}\right)^2 T_r + T_{amb_m} \quad (6)$$

Where:

A_m = the measured load in Amperes

A_r = rated load in Amperes

T_r = rated temperature rise from standards in ($^{\circ}\text{C}$)

T_{amb_m} = measured ambient temperature in ($^{\circ}\text{C}$)

Research by Epperly et al. [2] suggested that IRT can be used for condition monitoring of overhead lines, switchgear, capacitor banks, motor performance, transformers etc. Chudnovski [38] suggested that IRT can be used to monitor overheating of electrical components induced by corrosion and is often used in paper and pulp industries. Recent technological advances in the field of solid state and integrated circuits resulted in the widespread use of Printed Circuit Boards (PCBs) in which millions of electrical components are fabricated in a relatively small surface area having multiple onboard power supplies and a large number of electrical junctions. These junctions are potential sites of faults and identification of these faults in real time are essential for the proper functioning of the PCBs. Vishwakarma et al. [39] suggested that IRT can be used for the identification of these faults using the thermal anomalies across the board.

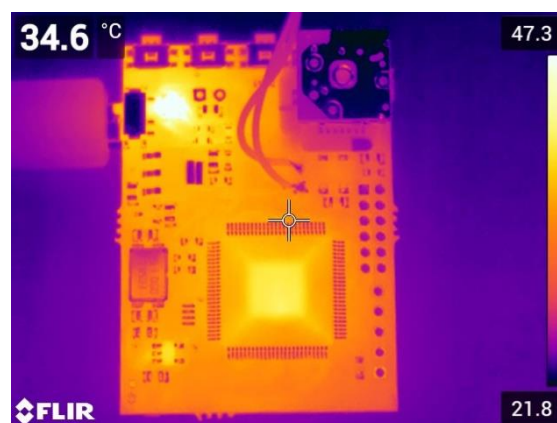


Figure 2. 6. Heat image of a PCB [39]

Wiecek et al. [40] used an active thermography technique to deduce the thickness of soldering done on PCB boards. They used an infrared light source to measure the backside irradiation from the PCB with an infrared camera. Different soldering shows different thermal characteristics because of the difference in conductivity and capacitance. These differences in thermal behavior were analyzed to measure the thickness of solders. Breitenstein et al. [41] used a high-speed infrared camera to detect the leakage sites in the ICs by a special technique called the lock-in thermographic system. They used a combination of a high definition microscope objective and a high-speed infrared camera to measure the leakage current and other heat sources on electronic boards and successfully measured temperature difference as low as 10 μ K and a spatial resolution of 5 μ m.

IRT has also been used extensively for CM of machines in industries. Loosely connecting bolts, stator misalignments, improper lubrication, overheating of machine components, wear out machine parts due to frictional force, overloading etc. have been supervised with IRT. Raišutis et al. [42] discussed various NDT techniques for inspection of wind turbines which includes vibration analysis, x-ray imaging, and IRT. They inspected the thermal behavior of the wind blades by applying a controlled thermal load on the blades. The thermodynamic properties of the materials then produced different surface temperature signatures which were analyzed to predict the condition of the blades. J.M. Karjanmaa used IRT to do CM of paper finishing machines [43]. Fairlie et al. used IRT for online temperature monitoring in hot-rolling of aluminum [44]. Leemans et al. [45] used IRT for condition monitoring of a blower coupled to a 500 kW motor. They used an Infrared camera to acquire the thermal signatures and used an efficient autorecursive model to compensate for the variation of the process and ambient temperature. In [46] Gaberson highlighted the use of IRT to determine the energy loss due to misalignment in rotational machines. He concluded that misalignments and unbalance of the rotating device can cause up to 3% and 1% energy loss respectively. He also concluded that misalignments up to 2% can cause a significant temperature rise in components of rotating devices.

Bagavathiappan et al. [7] used IRT for condition monitoring of bearings, motor shaft, motor exhaust system of a nuclear ventilation system. They identified abnormal temperature rise at the bearing and the shaft at the impeller end of the blower due to a defect in the gland packing. Further, they noticed an abnormal temperature rise at the pulley-drive system due to overtightening of bolts. The figures below show the temperature profile under the normal working condition and under the effect of the fault. The abnormal temperature rise (encircled region) in the later was attributed due to the improper gland packing.

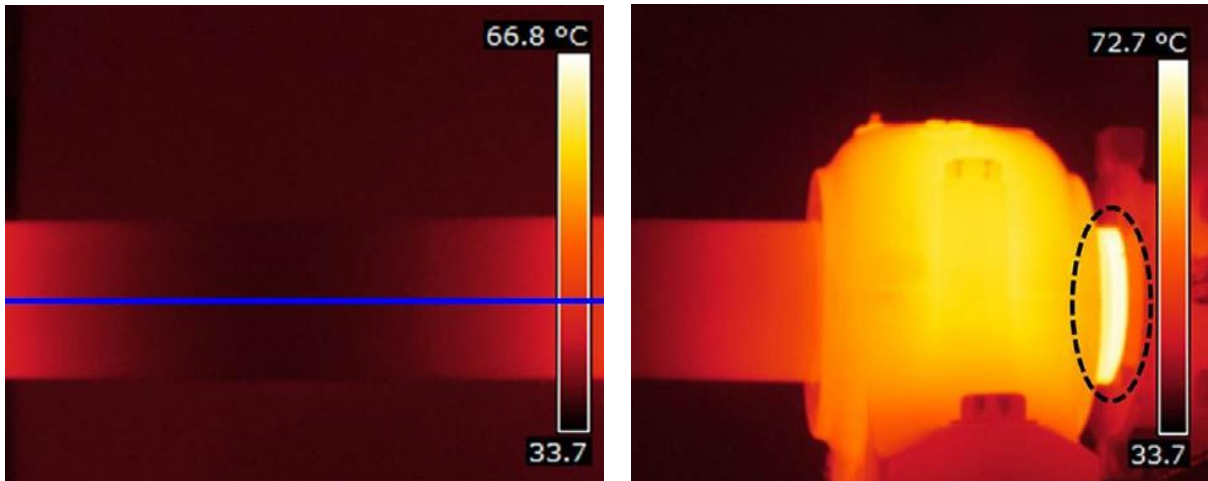


Figure 2. 7. (a) Heat profile under normal working condition. (b) Heat profile due to improper gland packing [7]

2.2.5. Conclusion

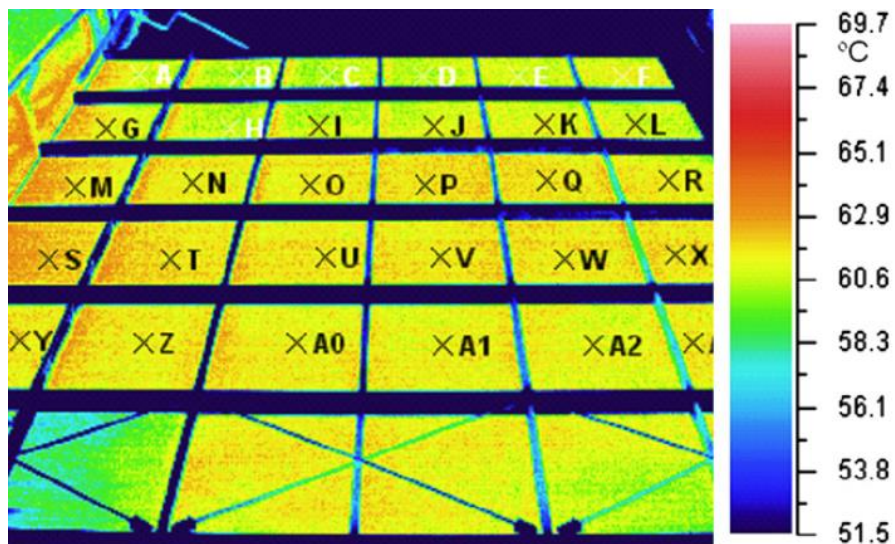
From the above section, it has become quite clear that IRT has been a very trusted tool and is used extensively in the various field for CM. Starting from civil structures monitoring to heating systems, industrial machinery to solid state microelectronic boards, nuclear power plants to aerospace industries, IRT has been very effective when it comes to real-time temperature measurement and CM in a non-contact way. Not only that, heat signature of a device provides pertinent information regarding the health and lifetime of device or equipment and thus IRT becomes very crucial to prevent a shutdown or avoid catastrophic breakdown.

But every system has its disadvantages too. IRT, though a very reliable source for CM but data acquisition from thermal cameras depends on several external factors which are often not taken into account leading to misinterpretation of machine condition.

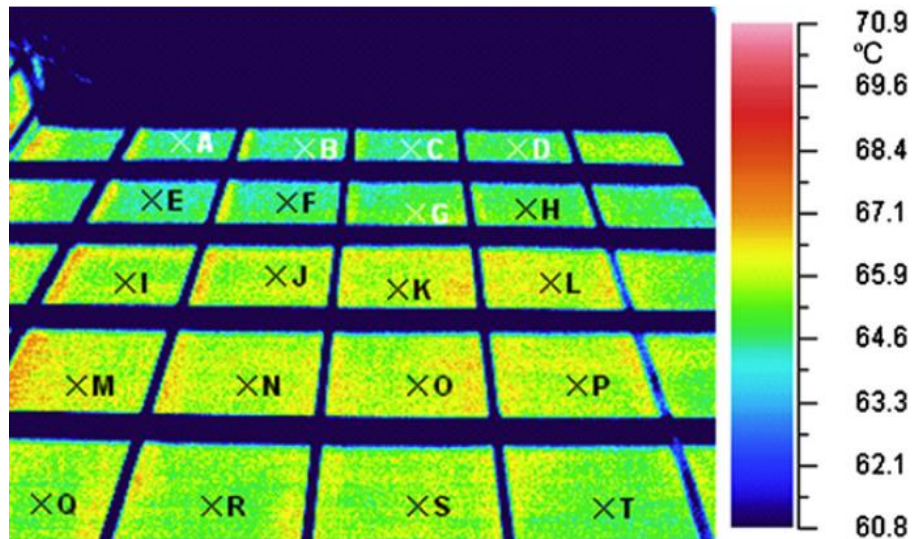
2.2.6. Problems related to Condition monitoring with IRT

As mentioned before external factors including ambient temperature, the speed of the wind, the emissivity of materials, energy reflected from surrounding surfaces affects thermal data and are some of the key factors that lead to inaccuracy in CM.

In [47] Ge et al. performed CM of direct air-cooled power generating units using IRT. They selected a direct air-cooled power generating system as the research object and inspected the distribution of heat on the surface due to the air-cooled condenser. Based on the monitoring results they formulated that the outer surface of the ACC units are prone to freezing in the winters although it was not the case. They concluded that ambient temperature has a profound effect on the thermal data and that the heat profile of the ACC units varies rapidly from season to season.



(a)



(b)

Figure 2. 8. Heat distribution profile of the ACC units. (a) Under the windless condition in winters. (b) Under windy conditions in summer [47]

The above figures represent the heat distribution on the ACC units at two different seasons of the year. They noted that the average surface temperature of the upstream ACC units was almost the same while the surface temperature of the sixth row under similar condition and same fan speed was about 3 °C higher. This was recorded during the winters with a wind speed of 1,8 m/s. During the summer, the environmental wind flowing horizontally over the ACC surface with a speed of 5,6 m/s, and the vertical exhaust air flow from the ACC condenser creates a vortex over the ACC surface. The ACC unit, under the same condition as in winter, shows a temperature difference of about 1 °C. Frate et al. in [15] showed how the wind speed and direction of wind affect thermographic data. He showed that change in direction of wind and change in wind speed vastly influence the accuracy of thermal data and thus the quality and process of measurements taken, is of great importance.

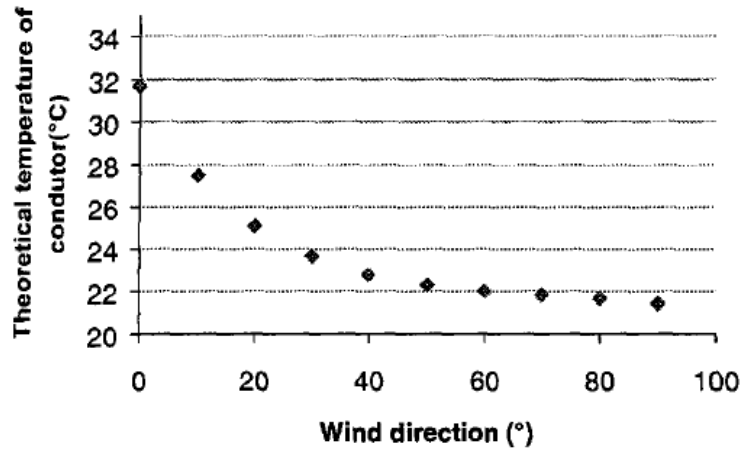


Figure 2. 9. Effect of wind speed on temperature measurement [15]

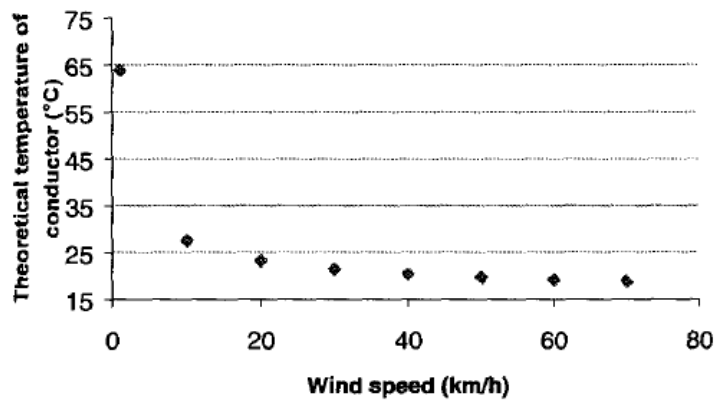


Figure 2. 10. Effect of wind direction on temperature measurement [15]

The above figures show how temperature measurements vary with varying wind speed and directions. It is to be noted that both the above measurements were taken at similar conditions (ambient temperature at 15 °C, a load of 600 A, emissivity $e = 0,5$). Ball et al. [48] performed rigorous investigations and suggested that thermographic measurements are subjected to errors due to certain factors like

- a). Incorrect Emissivity of materials
- b). Increased viewing distance causing excessive increasing of pixel areas.
- c). Atmospheric conditions like the scattering of suspended particulate or absorption of gasses.

Manuel et al. in [14] created an isothermal simulated environment to test the effect of energy radiated from surrounding heat sources on Thermographic camera measurements. They showed how the presence of heat sources in the vicinity of the thermal camera and the target object infuse errors in the thermal data. In [13] Martinez et al. hypothesized that ambient temperature has an adverse effect on data acquired through the thermal camera and that the corrected maximum allowable temperature for any electrical component is a function of ambient temperature. In [49] Jadin et al. mentioned that ambient temperature has an adverse effect on condition monitoring with IRT. L. dos. Santos et al. in [50] mentioned the difficulties encountered while evaluating thermal data measurements obtained from uncovered power substations. They emphasized the fact that under open air, fluctuations in ambient temperature induced erroneous readings from the thermal camera.

2.2.7. Conclusion

From the above section, it is clear that CM with IRT has its disadvantages too considering the fact that it produces errors depending upon ambient conditions like temperature, the presence of moisture, wind speed, and direction, the presence of heat source around the research object, solar temperature etc. Researches have been done in the past to address many of these factors. With new technologies and advanced image processing systems some of the factors have been nullified. For example, a quantitative data analysis often produces many accurate results and is much less prone to ambient conditions. But as mentioned in [17] qualitative data analysis is a fast process and requires less frequent monitoring than the quantitative methods and thus industries across the world prefer data monitoring in a qualitative manner.

Thus the effect of ambient temperature is something that hasn't been worked on and still is an area that is needed to be addressed in CM of machines with IRT.

3. RESULTS AND ANALYSIS

3.1. Overview

This section gives an overview of the simulation for the thermal data acquisition using the Infrared camera. It starts with the experimental set-up giving detailed information about the simulated environment developed for acquiring the temperature value of the motor bearing. This is followed by the results obtained at various ambient temperatures and finally, an analysis has been drawn to show the dependency of ΔT on ambient temperature. The chapter ends with the limitations and challenges faced in the research work and finally, a conclusion has been drawn with a possibility of further development on this particular field.

3.2. Experimental Set-up

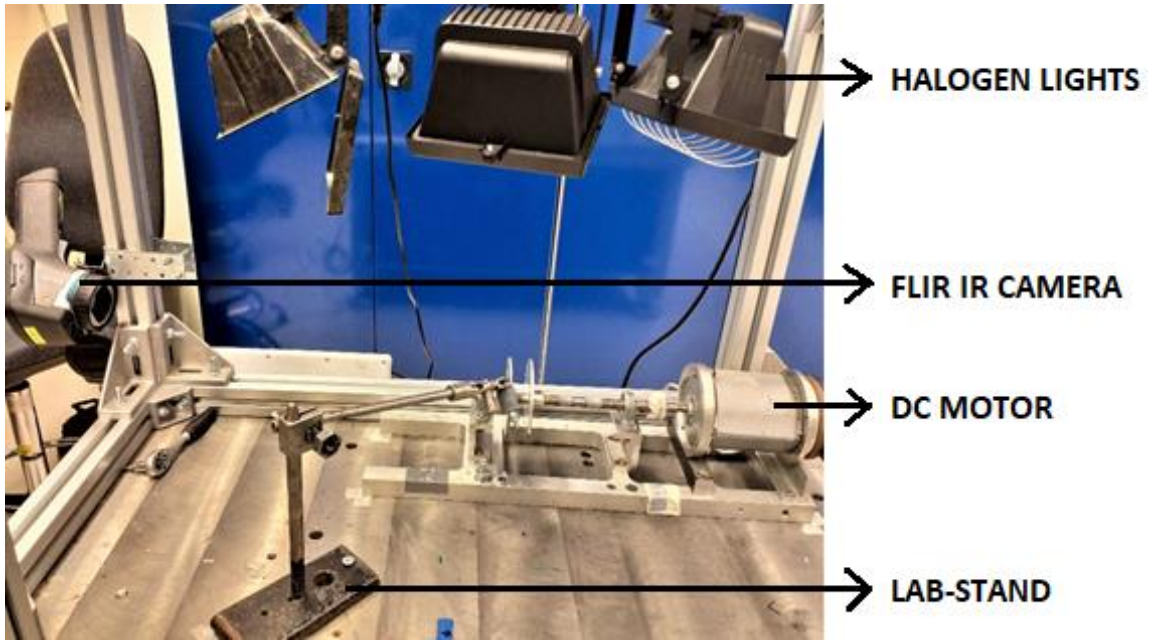
The simulation as shown in figure 3.2 was carried out with the Forward Looking Infrared camera (FLIR E50 Series) with an IR resolution of 240 x 180 pixels, a thermal sensitivity of $< 0,05$ °C, a field of view (FOV) of $25^\circ \times 19^\circ$, and a minimum focus distance of 0,4 m, a DC motor was selected as the research object, a lab-stand was used as an external load which represents an unpredicted load in the real world, a Fluke IR thermometer with a temperature measurement range of -30 to 500 °C and an accuracy of $\pm 1,5\%$ of reading, was used to record the ambient temperature, and three Halogen lights each of 500 W were used to increase the ambient temperature of the simulated area. The entire set-up was mounted on a polished tempered iron platform. The reason for choosing the platform was, that a tempered iron with a polished surface has a low emissivity (about 0,28) and hence the radiated energy from the surrounding surface is low, thus less interfering with the thermal data that is acquired through the IR camera. The focus was to remain entirely on the bearing of the motor where the ROI is located. The camera was mounted from the side of the platform at a distance of 0,5 m from the

motor which is above the minimum focus distance of the camera and was adjusted such that it focuses on the motor bearing only. The bearing which is made of stainless steel has an emissivity of 0,65-0,85 (see Appendix B.2), a value well suited for precise temperature measurement.

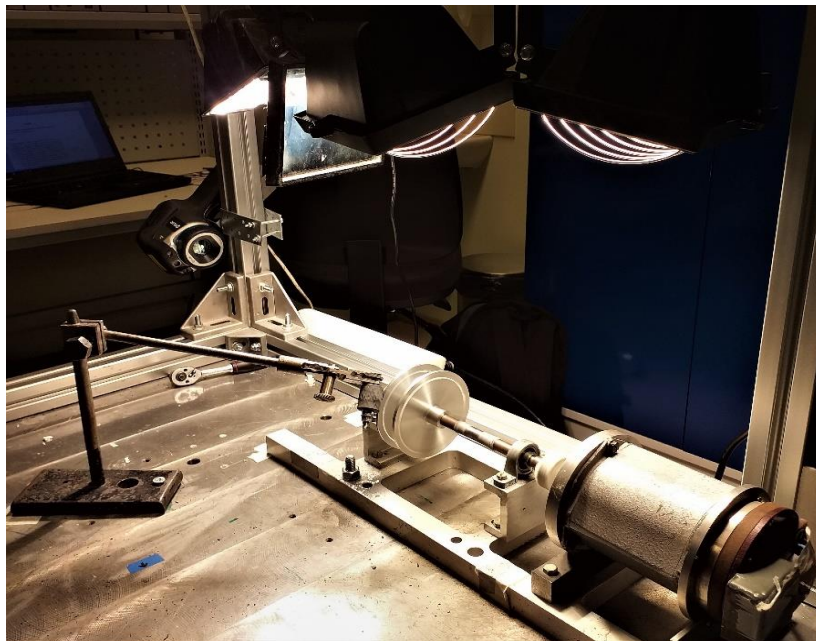


Figure 3. 1. (a) FLIR E50 Thermal Camera [51]. (b) FLUKE IR Thermometer [52].

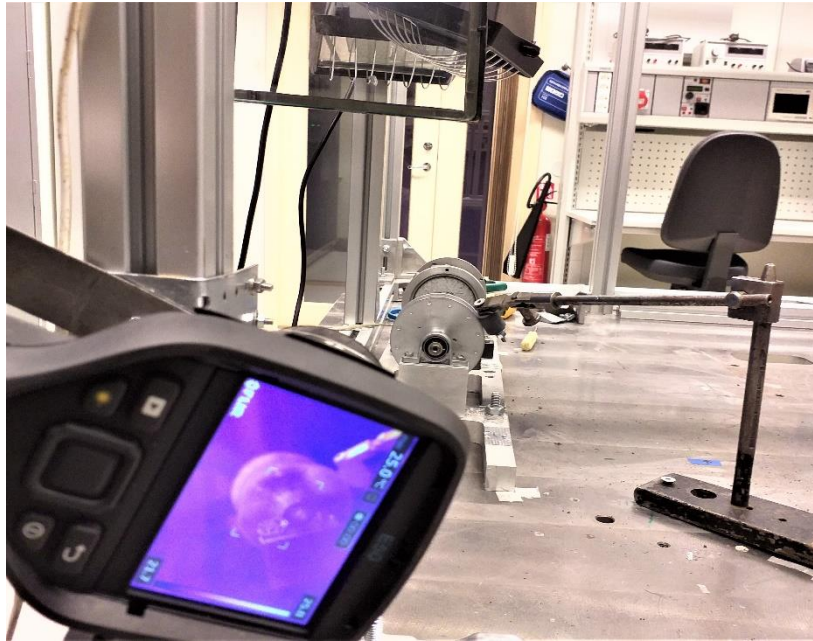
The figure below shows the simulation area for the thermal data acquisition with the FLIR IR Camera. The DC motor and the lab-stand was fixed with the iron platform to reduce vibration. The three halogen lights were fixed on the top of the platform to increase the volume of the heating area. For the accuracy of the simulation, it would have been ideal to create an isothermal system rather than an open system although the overall temperature variation at each ambient temperature achieved, was more or less stable. The camera was attached on the side of the platform as shown in the figure. It was ensured that the position of the motor and the lab-stand do not change during the course of the experiments.



(a)



(b)



(c)

Figure 3. 2: Experimental Setup of the simulation in Laboratory

A machine in an industry is subjected to various types of loadings and environmental hazards which are not often accounted for. Various types of machine faults like loose mechanical joints, misalignment of bearings, poor lubrication, overload on machine shafts, over-speed, frictional wear producing flanks and thus corrosion are being encountered in real life which is not possible for manufacturers and industries to predict [53]. These types of faults reduce machine lifetime, creates energy-loss and thus proper maintenance of these faults has to be taken. As mentioned earlier IRT has been used for condition monitoring of machines since the early '80s [54]. Abnormal temperature rise at the faulty junctions is captured in a thermographic image which is then further analyzed thus making it relatively easy for industries to locate the fault and hence take necessary action. Thus IRT plays a vital role in maintenance work when it comes to monitoring machines at industries.

The main downside of this thesis work was to get a machine having a fault so that thermal data can be acquired for validation. The challenge was to create a simulated environment wherein a machine experiences an unpredicted load which is often the case in industries. The lab stand with a rubber shoe at the tip was used to create an environment wherein the machine is subjected to an unpredicted load. The idea was to create a frictional load on the machine and then to gather thermal data for further analysis. The amount of load that is being applied is relevant to the fact that it changes the

amount of heating and hence the temperature in each case. Thus it was ensured that the amount of applied load remained constant. The figure below shows the load that is applied to the motor. The shaft of the motor has two attached disks. An unbalanced disk would load the bearing thus generating heat. This principle was utilized to create the required load for the experiment. Initially, the disk unbalance was created by attaching nut bolts on it. But the problem was, as the weight of the bolts increases it causes the motor rack to vibrate at a high frequency which could potentially damage the machine or the motor. So the other option was to decrease the weight of the attached screws. But then again as the weight decreases the amount of loading on the bearing decreases which in turn decrease the temperature rise. It was noted experimentally that a load greater than 0,5 N was causing the rack to vibrate. Moreover, in real life, a machine in an industry experience loads far greater than this range. Thus it was decided that the load will be applied through the lab-stand with the motor and the lab-stand both being fixed to the iron platform, ensuring that the rubber shoe-tip just touches the disks at the same position each time as shown in figure 3.3.

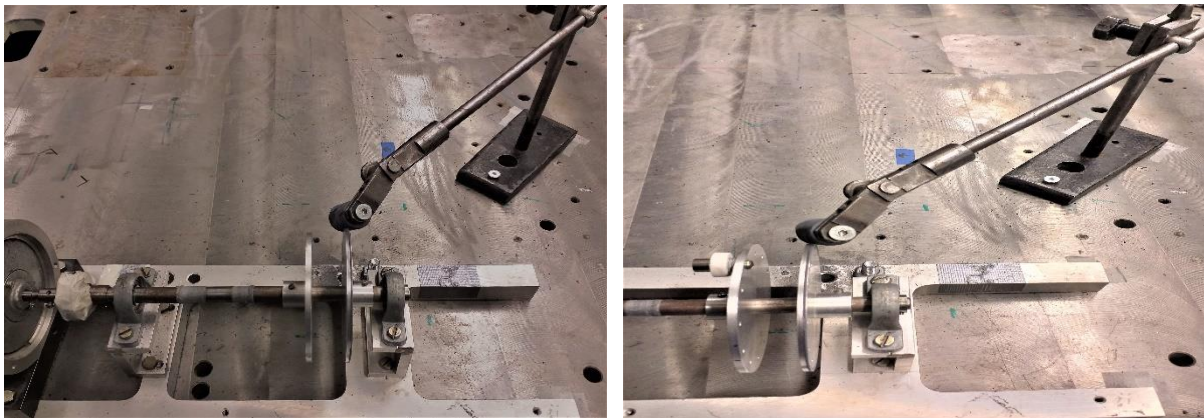


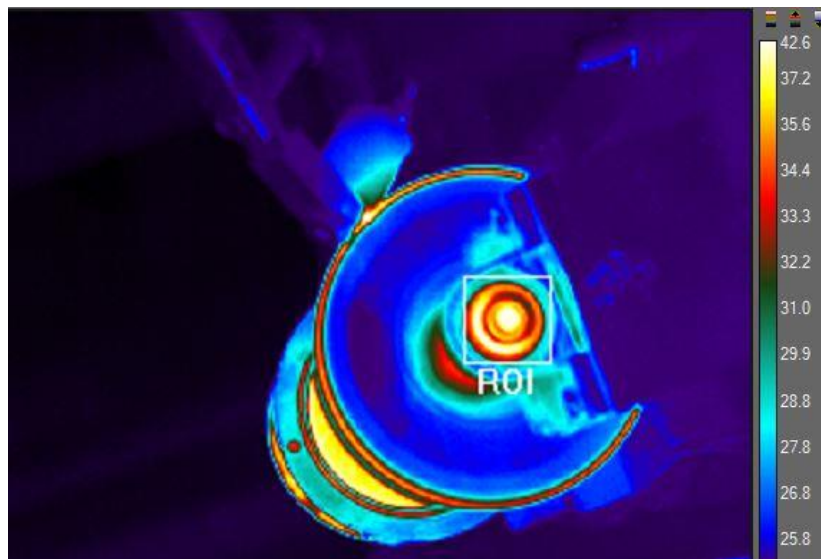
Figure 3. 3. Position of the lab-stand with rubber shoe just touching the disk on the motor shaft.

Now as the motor starts rotating the rubber shoe in the lab stand which is in contact with the disk creates a frictional force on the motor shaft which in turn loads the bearing. This unaccounted loading on the bearing led to a subsequent temperature rise which is then captured in real-time using the FLIR IR camera. The acquired data is monitored and analyzed using the FLIR ResearchIR Tool.

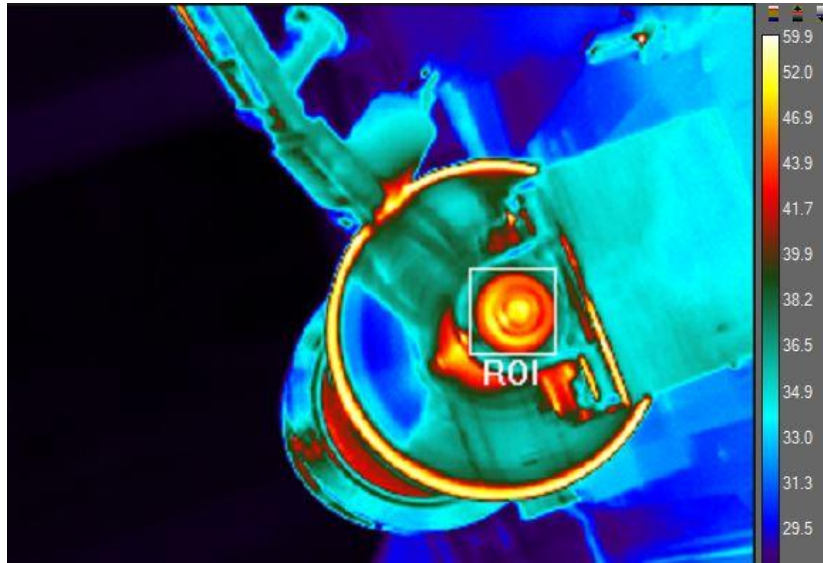
Data analysis for condition monitoring of electrical machines is generally done in two ways [49]. First, there is the quantitative data analysis where the temperature of the research subject or the equipment are directly acquired for analysis and the second method is the qualitative data analysis where a relative temperature value of the region of interest is compared to a reference region both

at similar conditions. Generally, industries prefer the qualitative data analysis as the process is fast, and does not require rigorous monitoring of the temperature signature of the hotspots [17].

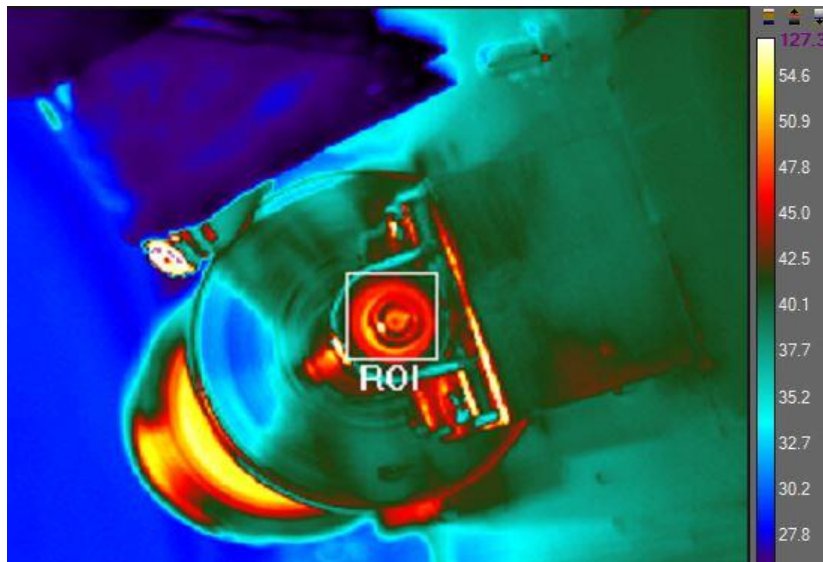
In this thesis work data analysis of the thermal signatures is done in a qualitative way wherein temperature difference of the bearing in loaded and unloaded conditions was compared, with the unloaded bearing temperature used as the reference temperature. The thermal data acquisition was done over a period of 15 minutes for each loaded and unloaded conditions at 3 different ambient temperatures, 23 °C which was the room temperature of the laboratory, 34,6 °C, and 41,2 °C. It is to be noted that the laboratory has controlled room temperature and thus the rise in temperature of the simulated area was getting saturated after a certain time interval. With two halogen lights on, the temperature of the simulation area was getting saturated at 34,6 °C and with three lights on, the maximum temperature that was possible to attain was 41,2 °C. Thus these 3 temperatures with $\pm 0,5$ °C as tolerance were selected as the test temperatures. The figure below shows the hotspot and the ROI at three different ambient temperatures. All the images were captured at the end of each experiment.



(a)



(b)



(c)

Figure 3. 4. Hotspots of the Thermography obtained from the Infrared Camera. (a) At 23 °C, (b) At 34,6 °C, (c) At 41,2 °C

The ROI in each of three cases is represented with the white bounding box. The bounding box covers the bearing of the motor. These images are taken at the end of each experiment and the screenshots represent the last frame in each case. From the images, it can be clearly seen how the bearing temperature increases with the application of load. The scale on the side maps the pixels value with temperature. The FLIR camera maps the RGB values of each pixel to a temperature scale. The acquired temperatures of the region of Image was recorded after every 1 minute for 15 minutes thus giving a total of 15 readings for the loaded and unloaded conditions at each ambient temperatures. The tables below show the acquired thermal data at each respective temperatures.

3.3. Results

Table 3. 1. Thermal Data at 23 °C

TIME (min)	ACQUIRED TEMPERATURES (°C) (at 23 °C)		$\Delta T = (\text{loaded} - \text{unloaded})$ (°C)	MEAN ΔT $\Sigma (\Delta T/\Delta t)$ (°C/min)
	Unloaded	Loaded		
1	25,8	25,9	0,1	4,781
2	34,2	36,7	2,5	
3	37,7	40,8	3,1	
4	39,5	42,1	2,6	
5	40,4	43,8	3,4	
6	41,2	44,9	3,7	
7	41,4	46,1	4,7	
8	41,9	46,8	4,9	
9	42	47,5	5,5	
10	42,2	48,1	5,9	
11	42,4	48,3	5,9	
12	42,9	48,9	6	
13	43,1	49,3	6,2	
14	42,9	50	7,1	
15	43	50,3	7,3	
16	43,1	50,7	7,6	

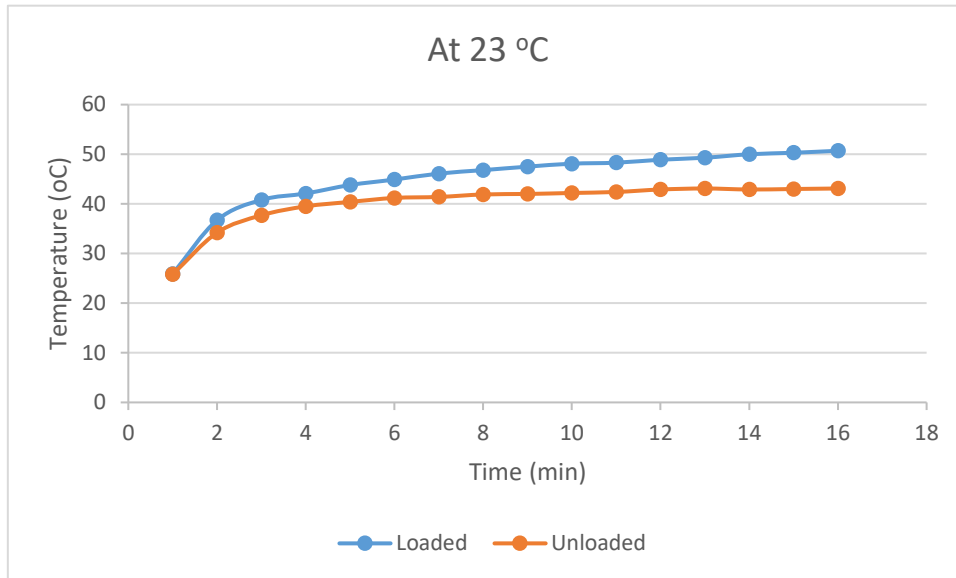


Figure 3. 5. Temperature gradient for the loaded and unloaded bearing at 23 °C

Table 3. 2. Thermal Data at 34,6 °C

TIME (min)	ACQUIRED TEMPERATURES (°C) (at 34,6 °C)		$\Delta T = (\text{loaded} - \text{unloaded})$ (°C)	MEAN ΔT $\Sigma (\Delta T/\Delta t)$ (°C/min)
	Unloaded	Loaded		
1	35,1	35,6	0,5	6,8125
2	42,1	45,1	3	
3	42,3	46,1	3,8	
4	42,3	47,1	4,8	
5	42,4	47,8	5,4	
6	42,8	48,6	5,8	
7	42,9	49,4	6,5	
8	43	50,1	7,1	
9	43,3	50,7	7,4	
10	43,3	51,4	8,1	
11	43,5	52	8,5	
12	43,9	52,9	9	
13	44,4	53,7	9,3	
14	44,8	54,6	9,8	
15	45,2	55	9,8	
16	45,6	55,8	10,2	

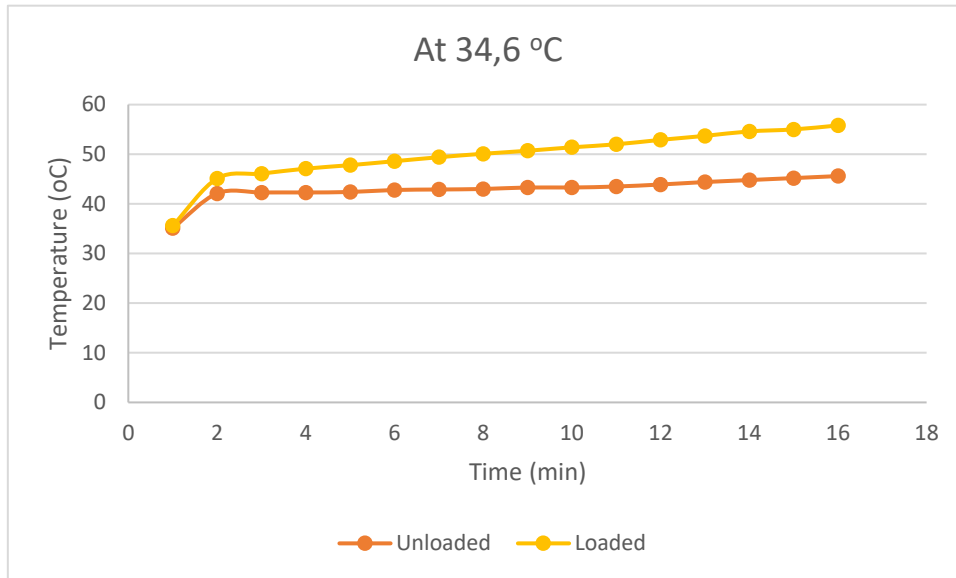


Figure 3. 6. Temperature gradient for the loaded and unloaded bearing at 34,6 °C

Table 3. 3. Thermal Data at 41,2 °C

TIME (min)	ACQUIRED TEMPERATURES (°C) (at 41,2 °C)		$\Delta T = (\text{loaded} - \text{unloaded})$ (°C)	MEAN ΔT $\Sigma (\Delta T/\Delta t)$ (°C/min)
	Unloaded	Loaded		
1	42,1	43	0,9	8,2562
2	50,1	55,8	5,7	
3	51,2	56,9	5,7	
4	51,4	58	6,6	
5	51,4	59,1	7,7	
6	51,6	59,6	8	
7	52	60	8	
8	52,1	60,6	8,5	
9	51,8	60,7	8,9	
10	52,2	61,2	9	
11	52,6	61,9	9,3	
12	53	62,7	9,7	
13	53,1	63,2	10,1	
14	53,2	64	10,8	
15	53,6	64,9	11,3	
16	53,4	65,3	11,9	

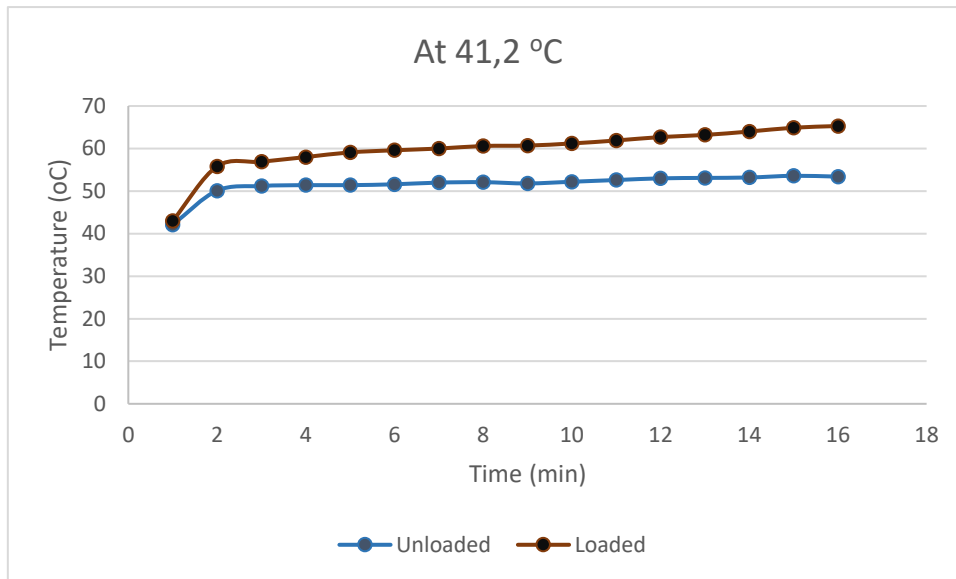


Figure 3. 7. Temperature gradient for the loaded and unloaded bearing at 41,2 °C

From the above tables it can be clearly seen that as the ambient temperature increases, it increases the temperature of the bearing within the ROI although the rate of increase of temperature in each of the 3 cases is different for the loaded and unloaded conditions. If we take out the ambient temperature out of the equation, all prevailing conditions remained almost the same during each experiment. It is to be noted that after each experiment it was ensured that the motor cools down to its normal temperature before acquiring the next set of data.

The rate of increase of the temperature differential ($\Delta T/\Delta t$) of the ROI between the loaded and unloaded bearings increases with the increase in ambient temperature. This ΔT is considered to be the main parameter when it comes to qualitative analysis of thermal data [55]. It should be kept in mind that this increase in $\Delta T/\Delta t$ is achieved after 15mins of machine on-time. Various International standards exist which provides such ΔT tables for qualitative measurement of thermal data. Some of the commonly used standards are International Electrical Testing Association (NETA) [30], American Society for Testing and Materials (ASTM) [31], National Fire Protection Association (NFPA) [32].

For classifying thermal anomalies for industrial machine monitoring several critical conditions are considered:

Table 3. 4. ΔT Specifications by the International Electrical Testing Association (NETA) Maintenance Testing Specification [30].

ΔT based on comparisons between similar components under similar loading.	ΔT based on comparisons between components and ambient air temperature.	Recommended Action
1 °C - 3 °C	1 °C - 3 °C	Possible deficiency; warrants investigations
4 °C - 15 °C	11 °C – 20 °C	Indicates probable deficiency; repair as time permits
---	22 °C - 40 °C	Monitor continuously until corrective measures can be accomplished
>16 °C	>40 °C	Major discrepancy; repair immediately

Table 3. 5. ΔT Specification by Recommendation for a manufacturer’s Motor Control Centres [33].

ΔT	Recommended Action
<10 °C	No Service/repair required
10 °C - 25 °C	Service at next maintenance schedule
25 °C - 50 °C	Immediate Service required and monitor unit at next maintenance schedule
>50 °C	Shutdown Unit and Repair

The figure below shows how ΔT increases with time at the respective ambient temperatures.

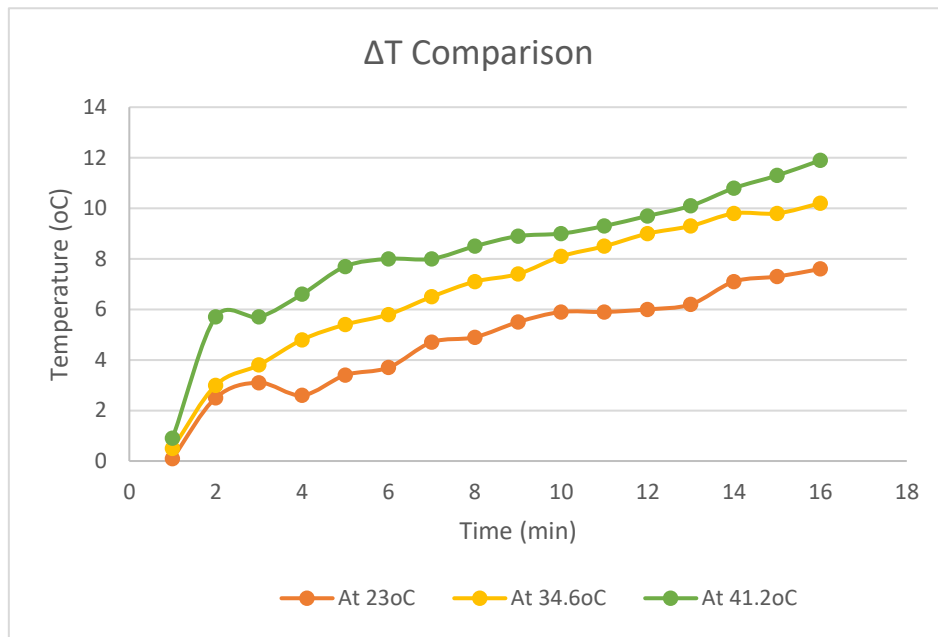


Figure 3. 8. Trend of ΔT at 3 different ambient temperatures

The graph above shows how ΔT changes with time as the ambient temperature increases. The thermal signature clearly shows that as the ambient temperature increases it increases the temperature difference between the loaded and unloaded bearing.

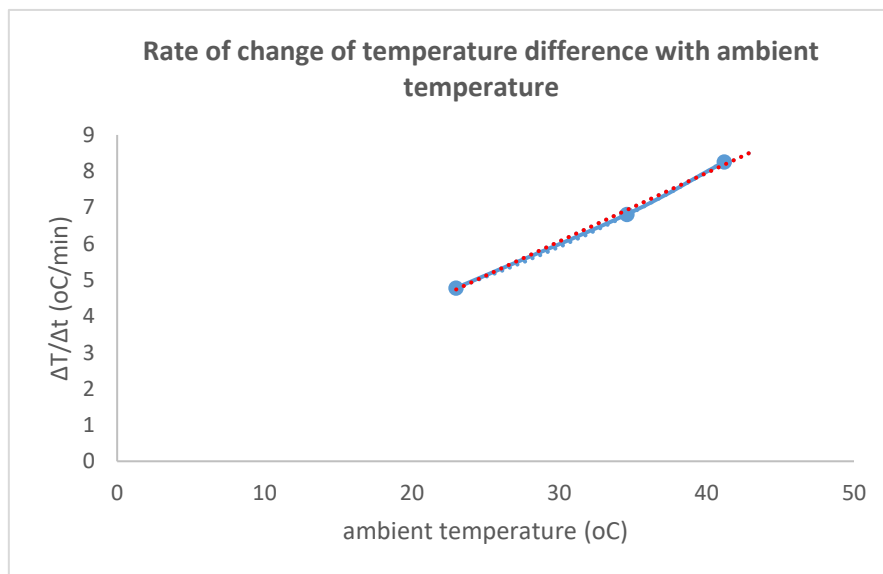


Figure 3. 9. Graph showing the relation between the 'rate of change of temperature' with 'ambient temperature'.

The above figure shows the graphical representation of how the rate of change in temperature differential varies with ambient temperature. As we can see that, the change in temperature differential varies linearly with the change in ambient temperature i.e. as ambient temperature increases, the temperature difference of the bearing, between loaded and unloaded condition, also increases. Now, from the curve, it can be seen that it is not exactly linear and that is down to the fact that several other factors influence this temperature difference. As hypothesized before this ΔT is not only proportional to the ambient temperature, but it is also affected by the amount of frictional force generated, in this case by the lab-stand, the torque generated by the motor shaft and the load currents applied at the motor.

$$\Delta T \propto \left(\tau_m, -F_k \Theta, \frac{Am}{Ar}, \varepsilon, T_{amb} \right) \quad (7)$$

Now considering all other factors to be constant apart from the ambient temperature we get

$$\frac{\Delta T}{\Delta t} \propto T_{amb} \quad (8)$$

$$\frac{\Delta T}{\Delta t} = k T_{amb} \quad (9)$$

Where 'k' is the proportionality constant or the slope of the straight line. Unit of 'k' is min^{-1} . As the unit of 'k' suggests it is equivalent to the inverse of time or frequency. Thus the rate of change of temperature difference between the selected ROI is proportional to the rate of change of ambient temperature or the frequency of the changing ambient temperature.

3.4. Limitations of the Thesis work

As with every research work this thesis work also had some limitations. Certain assumptions were made for the validity of the work.

- As hypothesized, the temperature difference of the bearing within the ROI is a function of several factors other than ambient temperature like the emissivity of materials, the frictional force applied, the load current, the torque generated by the motor shaft due to the applied load. For this thesis work, all these factors were assumed to be constant.
- The rubber-shoe attached with the lab-stand was used as an unpredicted load experienced by the machine, to simulate the load in the real world. With friction, the rubber-shoe was withering bit by bit. Thus with every experiment, the load, which was considered as constant, was decreasing. Although the amount of decrease in load was very negligible.
- Due to the controlled room temperature in the laboratory, it was difficult to attain a certain temperature and maintain it. With the halogen lights on, the temperature of the simulation area initially was increasing at a very high rate until it was getting saturated after a certain time duration. During the course of the experiments at each ambient temperature, the overall temperature was more or less constant with a variation of about $\pm 0,5$ °C.
- The bearing is made of stainless steel which has an emissivity in between 0,65-0,85. The FLIR ResearchIR tool has the provision of choosing the emissivity of the material under thermal analysis. For this thesis work, since the exact value of emissivity was unknown, it was assumed that the emissivity of the material was 0,65. The reason for choosing the lowest value was, as stated earlier ΔT increases with increase in the emissivity of the material, so the idea was to check whether it is true for the lowest value also.
- It was assumed that other environmental factors like humidity and wind flow within the laboratory remained constant during the course of the experiments.

3.5. Conclusion and Future work

It may be concluded from this research work that thermal data analysis, done in a qualitative manner for condition monitoring of machines varies linearly with ambient temperature. The thermal signature of the motor bearing changes with a change in ambient temperature under the effect of a constant load. It is to be noted that the findings of this research were entirely based on the particular motor used in this case. When it comes to industrial machines in the real world several other factors must be considered. Practically, machines in industries bear a load of much higher quantity which might affect the thermal behavior of the subject under study. Nevertheless, the aim of this thesis work was to find a relation between the rates of change of ΔT with the change in ambient temperature and as previous studies have suggested, the two variables are linearly proportional.

Thus industries using Infrared Thermography for monitoring machine performance has to take ambient temperature into account. Places, where the climatic temperature differs a lot from summer to winter, might face this problem more often than not. Thus industries situated in such areas have to take care of the ambient temperature within the workplace. Maintaining a constant temperature in the workplace is one solution.

Several factors other than ambient temperature affect condition monitoring with IRT. As mentioned before many of the areas like humidity, solar heating, and energy reflected from surrounding surfaces that affect CM, still needs to be addressed. In future, researchers might dig into some of these factors and hence find out how they actually affect qualitative thermal data analysis. The principal aim of these researches would be to increase the accuracy of predictions regarding machine conditions, lifetime and performance. Machine Intelligence is another way of increasing accuracy. Su et al. in [56] suggested a neural network model for monitoring Induction motor by analyzing vibrations. But as stated before vibration sensors are generally contact-type sensors and are difficult to install. So machine learning can be implemented for CM using IRT for modeling an efficient monitoring system capable of predicting faults at an early stage and hence provide early warnings.

4. SUMMARY

Condition monitoring of machines is an important aspect in industries as it prevents the process break down and unconditional shutdown, increases machine lifetime and performance, and thus prevent economic losses. Several condition monitoring processes like vibration analysis, acoustic emission detection, ultrasound detection, temperature monitoring, etc. exists till date and industries use one or another based on the available infrastructures. Among all these processes, temperature monitoring is considered to be most valuable for the fact that it predicts machine conditions with greater accuracy and is relatively cheap.

Several temperature monitoring sensors are used for condition monitoring but Infrared cameras are considered to be the most useful as it is a non-contact type sensor. The problem with contact type sensors is that they have to be installed and monitored manually at the monitoring site which leads to human exposure and moreover installing these sensors is often not feasible owing to the mechanical structures of machines.

Data acquired from Infrared cameras are subjected to variations due to several conditions like ambient temperature, the presence of moisture in the air, the emissivity of materials, wind speed, heat emitted from surrounding surfaces, etc. Variation in thermal data may lead to faulty predictions about machine condition and hence render the process inaccurate. This thesis work deals with the effect of ambient temperature on condition monitoring of machines with Infrared thermography.

A simulated environment was developed where a DC motor was subjected to an external unpredicted load at three different ambient temperatures. The loading causes the bearing temperature to rise which was acquired using the FLIR IR camera. Qualitative data analysis was done with the acquired thermal data for the loaded and unloaded condition at three separate ambient temperatures. It was observed that the temperature difference of the region of image (ROI) under the loaded and unloaded condition increases as the ambient temperature increases and this rate of increase is directly proportional to the rate of increase in ambient temperature. As it was hypothesized, ambient temperature does have an effect on qualitative data analysis used in industries for condition monitoring of machines.

The goal of this thesis work was to develop a simulated model to verify the effect of ambient temperature on condition monitoring of machines. The finding of this research will help industries to predict machine condition with much more accuracy. The importance of ambient temperature in condition monitoring is significant for the fact that ambient temperature is a variable parameter which we have no control over. In places where the climate temperature is warmer throughout the year the, ambient temperature becomes an important factor for condition monitoring simply because, the actual temperature of the component under study, increases which might lead to faulty predictions about machine conditions. Similarly, in colder places, the component temperature might fall below the threshold of detection even when the actual temperature may be potentially harmful.

KOKKUVÕTE

Masinate seisundi seire on oluline aspekt tööstuses, kuna see aitab ennetada protsessi rikkeid, tingimusteta seiskumist, suurendab masinate eluiga ja jõudlust ning aitab seeläbi vältida majanduslikku kahju. Erinevad seisundi jälgimise protsessid nagu vibratsioonianalüüs, mürataseme mõõtmine, ultraheli sageduse tuvastamine, temperatuuri seire jne on siiani kasutuses ning üks või teine tulenevalt olemasolevast infrastruktuurist tööstuses rakendatud. Kõigist nendest protsessidest peetakse temperatuuri seiret kõige väärtuslikumaks, kuna see ennustab masinate seisundeid suurema täpsusega ja on suhteliselt odav.

Seisundi seireks võib kasutada mitmeid temperatuuri jälgimise andureid, kuid infrapunakaamerat peetakse kõige kasulikumaks, kuna tegemist on mittekontaktset tüüpi anduriga. Kontakt-tüüpi andurite probleem on selles, et neid tuleb jälgimiskohas paigaldada ja jälgida käsitsi, mis tingib kokkupuudet inimesega ning lisaks sellele ei ole sageli andurite paigaldamine masinate ehituse tõttu teostatav.

Infrapunakaamerate salvestatud andmed varieeruvad sõltuvalt mitmest tingimusest, näiteks ümbritseva õhu temperatuur, õhuniiskus, materjalide emissioon, tuule kiirus, ümbritsevatelt pindadelt väljastatud soojus jne. Hälbed termilistes andmetes võivad põhjustada vigaseid prognoose masinate seisundi kohta ja seega muuta protsessi ebatäpseks. Käesolev uurimistöö tegeleb keskkonnatemperatuuri mõju seirega masinate seisundile kasutades infrapuna termograafiat.

Loodi simulatsioonikeskkond, kus alalisvoolumootori suhtes rakendati välist ettearvamatut koormust kolmel erineval ümbritseva keskkonna temperatuuril. Koormus põhjustab laagri temperatuuri tõusu, mis mõõdeti FLIR infrapuna kaameraga. Kvalitatiivne analüüs viidi läbi saadud soojusandmetega laadimise ja mahalaadimise seisundis kolmel erineval ümbritseval temperatuuril. Täheledatai, et temperatuuride vahe piirkondade pildil koormatud ja koormamata seisundis tõusis ümbritseva õhu temperatuuri tõustes.

REFERENCE

1. Eti, M.C., S. Ogaji, and S. Probert, *Reducing the cost of preventive maintenance (PM) through adopting a proactive reliability-focused culture*. Applied energy, 2006. **83**(11): p. 1235-1248.
2. Epperly, R.A., G.E. Heberlein, and L.G. Eads. *A tool for reliability and safety: predict and prevent equipment failures with thermography*. in *Petroleum and Chemical Industry Conference, 1997. Record of Conference Papers. The Institute of Electrical and Electronics Engineers Incorporated Industry Applications Society 44th Annual*. 1997. IEEE.
3. Lindquist, T., L. Bertling, and R. Eriksson. *Estimation of disconnecter contact condition for modelling the effect of maintenance and ageing*. in *2005 IEEE Russia Power Tech, PowerTech; St. Petersburg; 27 June 2005 through 30 June 2005*. 2005.
4. M.R. Clark, D.M.M., M.C. Forde, *Application of infrared thermography to the non-destructive testing of concrete and masonry bridges*. NDT & E International, June 2003. **36**(4): p. 265-273.
5. Badulescu, C., et al., *Applying the grid method and infrared thermography to investigate plastic deformation in aluminium multicrystal*. Mechanics of Materials, 2011. **43**(1): p. 36-53.
6. Huth, S., et al. *Lock-in IR-thermography-A novel tool for material and device characterization*. in *Diffusion And Defect Data Part B Solid State Phenomena*. 2002. Citeseer.
7. Bagavathiappan, S., et al., *Condition monitoring of exhaust system blowers using infrared thermography*. Insight-Non-Destructive Testing and Condition Monitoring, 2008. **50**(9): p. 512-515.
8. de Brito Filho, J.P. and J.R. Henriquez, *Infrared thermography applied for high-level current density identification over planar microwave circuit sectors*. Infrared Physics & Technology, 2010. **53**(2): p. 84-88.
9. Kiiskinen, H.T., et al., *Infrared thermography examination of paper structure*. Tappi journal, 1997. **80**(4): p. 159-162.
10. Gowen, A., et al., *Applications of thermal imaging in food quality and safety assessment*. Trends in food science & technology, 2010. **21**(4): p. 190-200.
11. Black, J.E. *Thermal baseline factors in nuclear power plants*. in *Thermosense XI: Intl Conf on Thermal Infrared Sensing for Diagnostics and Control*. 1989. International Society for Optics and Photonics.
12. Menaka, M., et al., *Characterisation of adhesively bonded laminates using radiography and infrared thermal imaging techniques*. Insight-Non-Destructive Testing and Condition Monitoring, 2006. **48**(10): p. 606-612.

13. Martínez, J., R. Lagioia, and S. Edenor. *Experience performing infrared thermography in the maintenance of a distribution utility*. in *19th International Conference on Electricity Distribution, Vienna*. 2007.
14. Manuel, M.C.E., et al., *Errors in Thermographic Camera Measurement Caused by Known Heat Sources and Depth Based Correction*. *International Journal of Automation and Smart Technology*, 2016. **6**(1): p. 5-12.
15. Frate, J., et al. *Evaluation of overhead line and joint performance with high-definition thermography*. in *Transmission and Distribution Construction, Operation and Live-Line Maintenance Proceedings. 2000 IEEE ESMO-2000 IEEE 9th International Conference on*. 2000. IEEE.
16. Snell, J.R. and R.W. Spring. *The new approach to prioritizing anomalies found during thermographic electrical inspections*. in *Thermosense XXV*. 2003. International Society for Optics and Photonics.
17. Bagavathiappan, S., et al., *Infrared thermography for condition monitoring—A review*. *Infrared Physics & Technology*, 2013. **60**: p. 35-55.
18. Nandi, S. and H.A. Toliyat. *Fault diagnosis of electrical machines-a review*. in *Electric Machines and Drives, 1999. International Conference IEMD'99*. 1999. IEEE.
19. Vas, P., *Parameter Estimation, Condition Monitoring, and Diagnosis of Electrical Machines (Monographs in Electrical and Electronic Engineering)*. 1993: London, UK: Oxford Univ. Press.
20. Yazici, B., et al. *An adaptive, on-line, statistical method for bearing fault detection using stator current*. in *Industry Applications Conference, 1997. Thirty-Second IAS Annual Meeting, IAS'97., Conference Record of the 1997 IEEE*. 1997. IEEE.
21. Kliman, G., et al. *A new approach to on-line turn fault detection in AC motors*. in *Industry Applications Conference, 1996. Thirty-First IAS Annual Meeting, IAS'96., Conference Record of the 1996 IEEE*. 1996. IEEE.
22. Penman, J., et al., *Detection and location of interturn short circuits in the stator windings of operating motors*. *IEEE transactions on Energy conversion*, 1994. **9**(4): p. 652-658.
23. Tandon, N. and A. Choudhury, *A review of vibration and acoustic measurement methods for the detection of defects in rolling element bearings*. *Tribology international*, 1999. **32**(8): p. 469-480.
24. Márquez, F.P.G., et al., *Condition monitoring of wind turbines: Techniques and methods*. *Renewable Energy*, 2012. **46**: p. 169-178.
25. Juengert, A. and C.U. Grosse, *Inspection techniques for wind turbine blades using ultrasound and sound waves*. *Non-Destructive Testing in Civil Engineering*, 2009.
26. Yonghui, Y., et al., *An integrated on-line oil analysis method for condition monitoring*. *Measurement Science and Technology*, 2003. **14**(11): p. 1973.

27. Schoen, R.R., et al., *An unsupervised, on-line system for induction motor fault detection using stator current monitoring*. IEEE Transactions on Industry Applications, 1995. **31**(6): p. 1280-1286.
28. Morando, L., *Measuring shock pulses is ideal for bearing condition monitoring*. Pulp Paper, 1988. **62**: p. 96-98.
29. Arndt, R.W., *Square pulse thermography in frequency domain as adaptation of pulsed phase thermography for qualitative and quantitative applications in cultural heritage and civil engineering*. Infrared Physics & Technology, 2010. **53**(4): p. 246-253.
30. *STANDARD FOR MAINTENANCE TESTING SPECIFICATIONS for Electrical Power Equipment and Systems*, A.N.S.I. (ANSI), Editor. 1997, InterNational Electrical Testing Association (NETA): USA.
31. ASTM, A.E., *Standard Guide for Examining Electrical and Mechanical Equipment with Infrared Thermography*. West Conshohocken, Pennsylvania, ASTM International, 2005.
32. *Recommended Practice for Electrical Equipment Maintenance*, N.F.P. Agency, Editor. 2006: Massachusetts.
33. Company, A.-B., *Service/Repair Guidance for Allen-Bradley Company Bulletin 2100/2400 in Motor Control Center Units Based on Field Temperature Analysis* 1993.
34. Ljungberg, S.A., *Infrared techniques in buildings and structures: Operation and maintenance*. Infrared methodology and technology, 1994. **7**: p. 211.
35. Azenha, M., R. Faria, and H. Figueiras, *Thermography as a technique for monitoring early age temperatures of hardening concrete*. Construction and Building Materials, 2011. **25**(11): p. 4232-4240.
36. Grinzato, E., *State of the art and perspective of infrared thermography applied to building science*. Infrared Thermography: Recent Advances and Future Trends, 2012. **9**: p. 200-229.
37. Newport, R., *Improving Electrical System Reliability with Infrared Thermography: Part 2*. 1999.
38. Chudnovsky, B.H., *Corrosion of electrical conductors in pulp and paper industrial applications*. IEEE Transactions on Industry Applications, 2008. **44**(3): p. 932-939.
39. R.k. Vishwakarma, V.M., M. Shahid, *Fault diagnosing of a high density electronic card employing multiple power supplies using infrared thermography*. Journal of Non destructive Testing and Evaluation, 2008. **7**: p. 28-31.
40. Wiecek, B., E. De Baetselier, and G. De Mey, *Active thermography application for solder thickness measurement in surface mounted device technology*. Microelectronics journal, 1998. **29**(4-5): p. 223-228.
41. Breitenstein, O., et al., *Microscopic lock-in thermography investigation of leakage sites in integrated circuits*. Review of scientific instruments, 2000. **71**(11): p. 4155-4160.
42. Raišutis, R., et al., *The review of non-destructive testing techniques suitable for inspection of the wind turbine blades*. Ultragarasas, 2008. **63**(2): p. 26-30.

43. Karjanmaa, J.-M. *Thermal imaging and paper-finishing machines*. in *Thermosense XV: An International Conference on Thermal Sensing and Imaging Diagnostic Applications*. 1993. International Society for Optics and Photonics.
44. Fairlie, M., et al. *On-Line Temperature Measurement In Hot Rolling Of Aluminum Using Infrared Imaging Systems*. in *Thermosense XI: Intl Conf on Thermal Infrared Sensing for Diagnostics and Control*. 1989. International Society for Optics and Photonics.
45. Leemans, V., et al., *Evaluation of the performance of infrared thermography for on-line condition monitoring of rotating machines*. *Engineering*, 2011(3): p. 1030-1039.
46. Gaberson, H.A. *Rotating machinery energy loss due to misalignment*. in *Energy Conversion Engineering Conference, 1996. IECEC 96., Proceedings of the 31st Intersociety*. 1996. IEEE.
47. Ge, Z., et al., *Performance monitoring of direct air-cooled power generating unit with infrared thermography*. *Applied Thermal Engineering*, 2011. **31**(4): p. 418-424.
48. Ball, M. and H. Pinkerton, *Factors affecting the accuracy of thermal imaging cameras in volcanology*. *Journal of Geophysical Research: Solid Earth*, 2006. **111**(B11).
49. Jadin, M.S. and S. Taib, *Recent progress in diagnosing the reliability of electrical equipment by using infrared thermography*. *Infrared Physics & Technology*, 2012. **55**(4): p. 236-245.
50. Dos Santos, L., et al. *Infrared thermography applied for outdoor power substations*. in *Thermosense XXX*. 2008. International Society for Optics and Photonics.
51. FLIR. 2018; Available from: <https://www.flir.eu/globalassets/imported-assets/image/e50.png>.
52. FLUKE. *FLUKE 62 MINI IR THERMOMETER*. Available from: <http://www.powerelectronics.itu.edu.tr/files/fluke62.pdf>.
53. Mba, D. and R.B. Rao, *Development of Acoustic Emission Technology for Condition Monitoring and Diagnosis of Rotating Machines; Bearings, Pumps, Gearboxes, Engines and Rotating Structures*. 2006.
54. Williams, R., *Monitoring the condition of machinery*. *Physics in Technology*, 1976. **7**(4): p. 166.
55. Y.C. Chieh, L.Y., *Automatic diagnostic system of electrical equipment using infrared thermography*. *Proceedings of International Conference on Soft Computing and Pattern Recognition*, 2009: p. 155-160.
56. Su, H. and K.T. Chong, *Induction machine condition monitoring using neural network modeling*. *IEEE Transactions on Industrial Electronics*, 2007. **54**(1): p. 241-249.
57. FLIR. *FLIR E50 Specification*. 2018; Available from: <https://www.flir.eu/support/products/e50#Specifications>.
58. FLUKE. *FLUKE 62 MINI INFRARED THERMOMETER - Specifications*. 2018; Available from: <http://www.powerelectronics.itu.edu.tr/files/fluke62.pdf>.

59. FLIR, *FLIR ResearchIR MAX Brochure*. 2018.
60. Company, M.I., *Table of Emissivity of various surfaces*.

APPENDICES

Appendix A.1



Figure A. 1. FLIR E50 IR CAMERA [51]

Table A. 1: FLIR E50 IR Camera Specifications [57]

IR Resolution	240 x 180 Pixels
Thermal Sensitivity	< 0,05 °C at +30 °C
Field of View (FOV)	25° x 19°
Minimum Focus Distance	0,4 m
Frame rate	60 Hz

Appendix A.2



Figure A. 2. FLUKE 62 MINI IR THERMOMETER [52]

Table A. 2. FLUKE 62 MINI IR THERMOMETER Specification [58]

Measurement Range	-30 °C to 500 °C
Accuracy	$\pm 1,5$ °C or $\pm 1,5\%$ of reading (whichever is greater)
Ambient Operating Range	0 to 50 °C

Appendix B

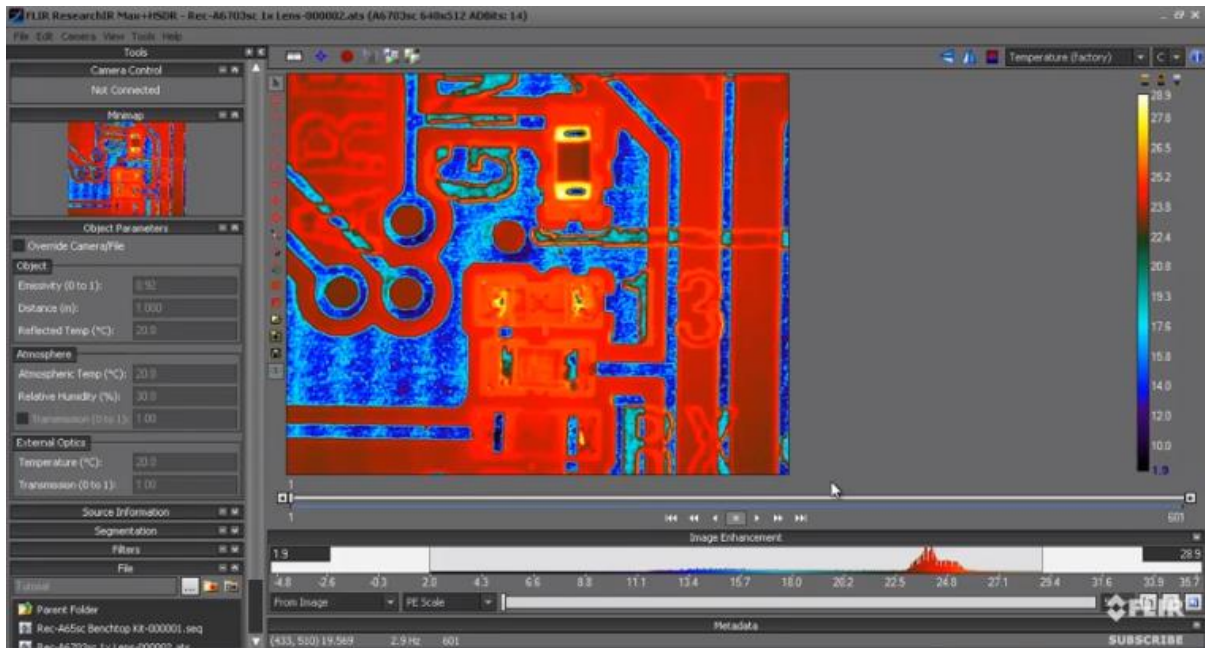


Figure B. 1. FLIR ResearchIR MAX: Analysis Tools [59]

Stainless Steel 18-8		
Buffed	20	0.160
Polished	93	0.16
.....	371	0.19
Oxidized.....	93-371	0.83
Stainless Steel 303.....	316	0.74
Oxidized.....	1093	0.87
Stainless Steel 304 (8Cr 18Ni)		
light silvery, rough brown,		
after heating	216-490	0.440-0.360
After 42 hours of heating at 527°C.....	216-527	0.620-0.730
Stainless Steel 310 (25Cr, 20Ni)		
Brown, splotched, oxidized from		
furnace service.....	216-527	0.900-0.970
Stainless Steel		
Allegheny metal No. 4, polished	100	0.130
Allegheny metal No. 66, polished	100	0.110
Steel		
Alloyed (8%Ni, 18%Cr).....	500	0.35
Aluminized	50-500	0.79

*When range of values for temperature and emissivity are given, end points correspond and linear interpolation of emissivity is acceptable.

Mikron Instrument Company, Inc.

Figure B. 2. Table of Emissivity of various Surfaces [60]